"AGC1-malate aspartate shuttle activity is critical for dopamine handling in the nigrostriatal pathway"

Irene Llorente-Folch[1], Ignasi Sahún[2], Laura Contreras[1], María José Casarejos[3], Josep María Grau[4], Takeyori Saheki[5], María Angeles Mena[3], Jorgina Satrústegui[1], Mara Dierssen[2], and Beatriz Pardo*[1]

[1] Departamento de Biología Molecular, Centro de Biología Molecular Severo Ochoa UAM-CSIC, and CIBER de Enfermedades Raras (CIBERER), Universidad Autónoma de Madrid, 28049-Madrid, Spain. [2]Programme of Genes and Disease, Center for Genomic Regulation, and CIBER de Enfermedades Raras (CIBERER), 08003, Barcelona, Spain. [3]Department of Neurobiology and CIBERNED, Hospital Ramón y Cajal, Carretera de Colmenar km 9,1, 28034-Madrid, Spain. [4]Department of Internal Medicine and Pathology, Hospital Clinic, University of Barcelona Medical School, Barcelona, Spain. [5]Institute of Resource Development and Analysis, Kumamoto University 2-2-1 Honjo, 861-0811 Kumamoto, Japan

***To whom correspondence should be addressed:**

Beatriz Pardo, PhD

Centro de Biología Molecular Severo Ochoa UAM-CSIC

and CIBER de Enfermedades Raras (CIBERER)

Universidad Autónoma de Madrid

28049-Madrid, Spain.

Email: bpardo@cbm.uam.es

Telephone: +34 91 196 4651

Fax: +34 91 196 4420

Abbreviations: AGC1, aspartate-glutamate carrier; COMT, catechol-*ortho*-methyl-transferase; DA, dopamine; DARP32, dopamine and cAMP regulated phosphoprotein of 32 KDa ; DAT, dopamine transporter; DOPAC, 3,4 dihydroxy-phenyl acetic acid; GSH, reduced glutathione; GSSG, oxidized glutathione; 5-HT, serotonin; HVA, homovanillic acid; MAO, monoamine oxidase; MAS, malate-aspartate shuttle; 3-MT, 3-methoxy-tyramine; NA, noradrenaline; NAA, N-acetylaspartate; SERT, serotonin transporter; Tyr, tyrosine; PD, Parkinson´s disease; PND, postnatal day; ROS, reactive oxygen species; TH, tyrosine hydroxylase; VMAT2, vesicular monoamine transporter 2.

ABSTRACT

The mitochondrial transporter of aspartate-glutamate Aralar/AGC1 is a regulatory component of the malate-aspartate shuttle. Aralar-deficiency in mouse and human causes a shutdown of brain shuttle activity and global cerebral hypomyelination associated with a drastic drop in brain aspartate and N-acetylaspartate levels. A lack of neurofilament-labelled processes is detected in the cerebral cortex, but whether different types of neurons are differentially affected by Aralar-deficiency is still unknown. We have now found that Aralar-knockout (Aralar-KO) mice show a general delay in neurodevelopment and unexpectedly, hyperactivity, anxiety-like behaviour and hyperreactivity. The striatum is the brain region most affected in terms of size, amino acid and monoamine content. The DOPAC/dopamine ratio specifically increases in striatum but no decrease in dopamine or in the number of nigral tyrosine hydroxylase-positive cells was detected in Aralar-KO brainstem. We find a fall in vesicular monoamine transporter-2 (VMAT2) levels associated with an increase both in non-vesicular dopamine and dopamine turnover through MAO activity. Our results suggest that Aralar-deficiency results in a failure to produce mitochondrial NADH and to an increase of ROS in the cytosol causing a fall in VMAT2 and GSH/GSSG ratio in striatum. The results indicate that the nigrostriatal dopaminergic system is a selective target of Aralar-deficiency.

Key words: malate-aspartate shuttle; AGC-1 deficiency; dopamine; global cerebral hypomyelination; VMAT2; OmniBank®

Running title: “Nigrostriatal pathway as a target for AGC-1 deficiency”

INTRODUCTION

Aralar is the brain isoform of the mitochondrial transporter of aspartate/glutamate mainly expressed in neurons (del Arco and Satrústegui, 1998; Ramos *et al*., 2003; Pardo *et al*., 2006, 2011) and its expression is increased during maturation in parallel to malate-aspartate shuttle (MAS) activity (Ramos *et al*., 2003). Aralar deficiency leads to a loss of respiration on malate plus glutamate, a shutdown of MAS activity, and a drop in brain and neuronal aspartate levels (Jalil *et al*., 2005). Neurons from Aralar-KO mice have a clear metabolic impairment in glucose oxidation due to the lack of a functional MAS, which results in an increased lactate production (Pardo *et al*., 2011). In intact cultured neurons, the maximal respiratory capacity of Aralar-KO neurons is clearly reduced as compared with control (Gómez-Galán *et al*., 2011), reflecting the limitation in pyruvate supply to mitochondria in the absence of a functional MAS.

Aralar-KO mice show a drop of N-acetylaspartate (NAA), hypomyelination, and a progressive failure to synthesise glutamine in brain astrocytes, suggesting that glutamatergic neurotransmission may be compromised in the older animals (Jalil *et al*., 2005; Pardo *et al*., 2011). These mice present motor problems, tremor, seizures and premature death (Jalil *et al*., 2005). Impaired development or degeneration of neuronal processes unrelated to myelin deficits has been observed in Aralar-KO mouse brain (Ramos *et al*., 2011). Besides, a study by Sakurai *et al.* (2010) showed that loss of functional Aralar leads to neurodevelopmental abnormalities in mice. On the other hand, in post-mortem brain samples from patients with autism, Aralar has been found upregulated in dorsolateral frontal cortex (Palmieri *et al*., 2008; Lepagnol-Bestel *et al*., 2008). And a strong linkage and association of the gene encoding Aralar, *SLC25A12*, with autism, a severe neurodevelopmental disease in humans, has been previously reported (Ramoz *et al*., 2004; Segurado *et al*., 2005; Turunen *et al*., 2007).

Recently, a patient with an homozygous loss of function mutation in *SLC25A12* was reported to show a loss of mitochondrial respiration on malate plus glutamate, low NAA levels, hypomyelination, arrested psychomotor development, hypotonia, and seizures (Wibom *et al*., 2009). These findings are important as the main features of aralar deficiency (reduced NAA levels and hypomyelination) are common in mouse and human, and support the importance of the Aralar-KO mouse for the study of the global cerebral hypomyelination (OMIM ID #612949). To gain insight into the targets affected in this early-onset brain disease, we have studied in more detail neurodevelopment, motor abilities and general behavior in Aralar-KO mice from postnatal day 1 (PND1) to PND22, analyzing neurochemical changes in specific brain areas of the Aralar-KO mouse.

Our data indicate that Aralar-KO mice show a delay in neurodevelopment and deficits in motor coordination, ataxic gait, altered geotaxia, increased reactivity, hyperactivity and anxiety-like behavior. Interestingly, we have found a pronounced decline in the levels of cathecolamines such as dopamine (DA) and serotonin (5-HT). The present results reveal a high susceptibility of DAergic neurons, specifically those DAergic groups of the nigrostriatal system, to Aralar-MAS dysfunction. A large body of evidence supports that nigrostriatal DAergic neurons are highly vulnerable to oxidative stress (Mena *et al*., 1993, 1997; Pardo *et al*., 1995; Canals *et al*., 2001), and to impairments of energy metabolism (Zeevalk *et al*., 1997; Pickrell *et al*., 2011). Our results evidence that the striatum is a preferential target of Aralar deficiency which leads to a lack of maturation of the GABAergic neurons and a reduction and mishandling of DA. Our results suggest a role of oxidative stress caused by Aralar deficiency as the origin of dopamine mishandling in striatum.

MATERIALS AND METHODS

Methods including animal housing and genotyping, postnatal observations in mice, neurobehavioral development and histomorphological studies of muscle are described in Supplementary material.

Brain regions and tissue preparation for amino acid analysis

Mice at PND19 were anesthetized, the whole brain was immediately removed from the skull and the brain regions were dissected according to Carlsson and Lindqvist (1973) and Itier *et al*. (2003) into the dopamine (DA)-rich limbic portion, the corpora striata (striatum), diencephalon, brain stem, cerebellum and cerebral cortex. Regions were sonicated in 3% perchloric acid (PCA), neutralized, and centrifuged at 10,000 x g for 15 min. Supernatants were lyophilized and dissolved in 0.2 M lithium citrate loading buffer pH 2.2 for quantification with an automatic amino acid analyzer Biochrom 20 (Pharmacia, Uppsala, Sweden) using a precolumn derivatization with ninhydrin and a cationic exchange column.

Measurements of monoamines in selected brain regions

The levels of DA and its metabolites, 3-methoxy-tyramine (3-MT), 3,4 dihydroxy-phenyl acetic acid (DOPAC) and homovanillic acid (HVA), noradrenaline (NA) and its metabolite, 4-hydroxy-3-methoxy-phenyl-glycol (MHPG), serotonin (5-HT) and its metabolite, 5-hydroxy-indole-acetic acid (5-HIAA) were measured by HPLC with an ESA coulochem detector, according to Mena *et al*. (1995). Briefly, samples from the same brain regions indicated above were sonicated in 8 volumes (w/v) of 0.4 N perchloric acid (PCA) with 0.5 mM $Na_2S_2O_5$ and 2% EDTA and then centrifuged for 10 min. Monoamine

levels were determined from 20 ul of the supernatant. The chromatographic conditions were: a column Nucleosil 5C18; the mobile phase, a 0.1 M citrate/acetate buffer, pH 3.9 with 10% methanol, 1 mM EDTA and 1.2 mM heptane sulfonic acid; and the detector voltage conditions: D1 (+0.05), D2 (-0.39) and the guard cell (+0.4).

Western blot in brain tissue

Aliquots (20 µg of protein) of brain lysates (in 20 mM Tris-HCl, 10 mM AcK, 1 mM DTT, 1 mM EDTA, protease inhibitor cocktail tablet (complete Mini, EDTA-free, Roche) 0.25% NP-40, pH 7.4) were centrifuged (12,000 x g, 30 min at 4 ºC) and electrophoresed in an 8% SDS acrylamide gel. Proteins were transferred electrophoretically to nitrocellulose membranes, which were blocked in 5% (w/v) dry skimmed milk (Sveltesse, Nestle) in Tris-buffered saline (10 mM Tris-HCl pH 7.5, 150 mM NaCl plus 0.05% (v/v) Tween-20) for 2 h, and further incubated with antibodies against Aralar (Del Arco and Satrústegui, 1998) (polyclonal antibody, 1:1000), dopamine markers (tyrosine hydroxylase, TH polyclonal antibody Millipore, 1:5000; dopamine transporter, DAT (SLC6A3) monoclonal antibody Millipore, 1:2000; vesicular monoamine transporter, VMAT2 (SLC18A2) polyclonal antibody Millipore 1:1000; dopamine and adenosine 3´, 5´-monophosphate-regulated phosphoprotein (32 kilodaltons), DARPP-32 polyclonal antibody Millipore 1:10000), glial markers (GFAP plyclonal antibody Dakopatts 1:500, for astrocytes; and OX-6 monoclonal antibody Serotec 1:500, for microglia), and β-actin (monoclonal antibody Sigma 1:10000), for 1 h at RT. Signal detection was performed with and enhanced chemiluminescence substrate (Western lighting-ECL; PerkinElmer).

Statistical analysis

For biochemical data, the statistical significance of the differences was assessed by One-way analysis of variance (ANOVA) followed by a *post hoc* Student's, Duncan/Tukey or Student-Newman-Keuls *t*-test method, as indicated. The results are expressed as mean ± standard error of the mean (s.e.m.).

RESULTS

General development, neurodevelopment, psychomotor state and motor coordination is altered in Aralar-KO mice

General development is delayed in Aralar-KO mice (Supplementary). Hyper-reactivity (**Fig. 1A-C**), spontaneous convulsions (**Fig.1B**) and tremor is observed in these animals (**Supplementary material**).

To evaluate the psychomotor state, social behaviour and motivations, we performed the homing test **(Fig. 1D).** The latency of Aralar wild-type (WT) mice to reach the opposite side of the cage stimulated by the presence of the nest was 7.2 ± 1.3 sec, showing high motivation to reach the goal. In contrast, Aralar-KO mice did not show any displacement toward the target during the test. Since the motor activity, measured in the openfield test (**Fig. 2),** seemed to be intact in Aralar-KO mice, the phenotype observed in the homing test may reflect reduced motivation and/or inability to initiate a voluntary motor response, one of the signs of basal ganglia dysfunction, particularly involving the caudate-putamen (Hauber, 1998; Palmiter, 2008).

In the acquisition of the surface righting response, WT mice improved the ability to upright from PND2 to 11 decreasing the latency from 7.0 ± 1.9 to 1.9 ± 0.04 sec at PND11. Aralar-KO mice reached similar latencies at mature stages, but showed a

significant impairment in early stages (**Fig. 3A**). This reflex depends on the development of dynamic postural adjustments and implies the integrity of muscular and motor function (Altman and Sudarshan, 1975; Dierssen *et al*., 2002). Acquisition of the negative geotaxis reflex (**Fig. 3C),** a dynamic test that depends on intact sensorimotor function (Dierssen *et al*., 2002), was also dramatically disturbed in KO mice. WT animals improved their performance along development, reaching latency times around 5 sec, while the KO mice were markedly impaired. Analogous results were found in the wire suspension reflex. The fine motricity of the forepaws does not appear to be affected in KO mice since this reflex was fully acquired, but significantly delayed in Aralar-KO mice (**Fig. 3B)**. All above-mentioned reflexes are sensitive to the function of the vestibular system, whose role is to provide information of the position and movement of the body and head in space (Altman and Sudarshan, 1975; for review, see Smith *et al*., 2005)**.** Regarding motor development, Aralar-KO mice showed a significant delay to acquire adult (walking) versus immature (pivoting) locomotor pattern compared with the WT siblings (**Fig. 3D).**

The results of the pawprint analysis showed a gait disturbance in Aralar-KO mice (**Fig. 4A, 4B)**. KO mice exhibited a significantly shorter stride length and hindpaw base width than their WT littermates (**Fig. 4A**), according to their smaller size, but presenting an erratic path (**Fig. 4B**). Beam balance test clearly demonstrated a motor impairment of Aralar-KO mice (**Fig. 4C)** who tended to lock in a fixed spastic posture while on the beam and almost all Aralar-KO mice fell off the bar. The delayed onset for the first movement in KO mice on the bar is near the maximum latency estimated in the task, 60 sec, while WT mice improved the performance in the second trial starting the movement in 26.5 ± 7.8 sec and reaching the end of the beam in 29.3 ±

7.5 sec. These motor deficits could be attributable to striatal dysfunction (Menéndez *et al*., 2006; Taylor *et al*., 2011) or increased anxiety/fear-related responses.

Thus, in Aralar-KO mice the neuromotor development is significantly delayed. KO mice showed a lack of motor coordination in the hindlimbs with no muscle affectation (**Figure S1**), sugestive of a failure in midbrian and/or forebrain structures.

Enhanced locomotor, exploratory activity and emotionality in Aralar-KO mice

The open field test, used to study motor activity and anxiety-related behavior in mouse (Carola *et al*., 2001), was assessed in two different environments, in low-lightening less aversive conditions (with red light) and in high-lightening aversive conditions (**Fig. 2**). Both WT and Aralar-KO were able to perform properly the task at PND15-16. Total distance travelled in low-lightening was statistically higher in Aralar-KO, with strong thigmotaxic behavior (preference to the periphery), compared with WT mice (**Fig. 2A)**, indicating a more anxious-like behavior. Aralar-KO mice were as fast as WT (mean speed, 8.7± 0.9 cm/sec; **Fig. 2B**), but with lower resting time (**Fig. 2C)** indicating hyperactivity. In the aversive (high-lightening) condition, Aralar-KO mice travelled significantly less distance in periphery than WT and than they did in low-lightening conditions (**Fig. 2A)**. Moreover, they showed a striking burst of speed in the centre of the arena (**Fig. 2B)**. Grooming and *fecal boli* in the high- vs. low-lightening condition were equally increased in all mice, however, the vertical activity (rearing), which involves hindlimb strength, tended to be higher in Aralar-KO mice in low-lightening condition than in WT mice (**not shown**), and this is also consistent with hyperactivity. These results indicate a rise in anxiety-, emotionality-related behaviors and reactivity in Aralar-KO animals.

Striatum is the main target for AGC1 deficiency

Although expression of Aralar-AGC1 has been extensively reported to be mainly restricted to and highly expressed in brain neurons (Ramos *et al*., 2003; Berkich *et al*., 2007; Xu *et al*., 2007; Cahoy *et al*., 2008; Pardo *et al*., 2011), no neuronal cell death in brain from Aralar-KO mice was detected (**not shown)**, but evident hypomyelination and loss of neurofilaments was reported occurring in specific brain regions (Jalil *et al*., 2005, Sakurai *et al*., 2010; Ramos *et al*., 2011). Aralar-KO mice have brain abnormalities consisting of a marked enlargement in brain lateral ventricles (**Fig. 5A**) (Jalil *et al*., 2005), also reported in human AGC-1 deficiency (Wibom *et al*., 2009). Figure 5 shows that the enlargement of lateral ventricles is related to a reduction in the size of striatum. Thus, the striatum/brain ratio size was significantly reduced to 80% in Aralar-KO mice versus WT (13.33 ± 0.04 % and 10.76 ± 0.03 % in WT and Aralar-KO, respectively; p = 0.0286); while the hippocampus/brain ratio size was unchanged (11.77 ± 0.02 and 12.74 ± 0.02 % in WT and Aralar-KO, respectively; **Fig. 5B**). Interestingly, the AGC1-deficient patient has also a smaller caudate-putamen than expected (Wibom *et al*., 2009).

Consistent with a preferential effect of Aralar deficiency in striatum, we found that the drop in whole brain Glutamine (Gln) content previously reported (Pardo *et al*., 2011) is more prominent in the striatum (**Table 1**) than in all the other brain regions analyzed, reaching 29% of WT levels in Aralar-KO mice. However, in cerebellum and particularly in brainstem Gln levels hardly drop, perhaps due to the presence of low levels of citrin, a component of malate-aspartate shuttle homologous to Aralar (Contreras *et al*., 2010). Striatal GABA was also significantly reduced to 60% in Aralar-KO **(Table 1)**, with no changes in all the other brain regions.

On the other hand, **Table 1** shows that none of the brain regions analyzed differed with respect to the drop in whole brain aspartate, serine and alanine levels (Pardo *et al*., 2011).

Thus, the striatum appeared to be the brain region most affected by aralar deficiency.

Monoamine metabolism is impaired in brain from Aralar-deficient mice

Given the marked inability of Aralar-KO mice to perform motor tasks and the hyper-reactivity, hyper-activity and anxiety observed in the tests performed, and the prominent effect of Aralar deficiency in the striatum, we decided to investigate the metabolism of monoamines in several brain regions, and particularly in striatum, as it is closely involved in the former functions (see Stein *et al*., 2006 for references).

NA content was similar in WT and Aralar-KO mice in any of the regions studied **(Table 2)**.

Regarding the serotoninergic system, Aralar deficiency resulted in a significant decrease both in 5-HT levels and specially those of its intracellular degradation product 5-HIAA in diencephalon (to 51% and 43%, respectively, versus control) and brainstem (to 72% and 59%, respectively) (**Table 2**), with similar changes in striatum and limbic system (**Table 2**), which have much lower 5HT content than the former areas. Of note, mRNA for serotonin transporter (SERT/Slc6a4), the plasma membrane transporter of serotonin which terminates the action of serotonin, is greatly increased (5.5-fold of WT value) in Aralar-KO brain (**Table S3**), suggesting that an increased reuptake of this neurotransmitter may be related to a reduced intracellular degradation of 5-HT to 5-HIAA through monoamine oxidase (MAO) activity and subsequent decrease in 5-HIAA/5HT ratio (**Table 3**) in brain from Aralar-KO mice.

In the brainstem, where the DAergic neuronal somata of the nigrostriatal pathway are located, no obvious change in the number of TH-positive cells was apparent. Neither the substantia nigra nor midbrain from Aralar-KO mice showed changes in TH-immunolabeling (**Fig. 5C, 5D**) or expression of TH (**not shown)** as compared to WT. Moreover, DA and its metabolites were increased or unchanged in brainstem and diencephalon, the major regions enriched in DAergic somata, from Aralar-KO mice (**Table 2**).

In contrast, Aralar deficiency resulted in changes in DA and its metabolites in the regions enriched in DAergic projections, striatum and limbic system. Aralar-KO striatum showed a substantial reduction in DA (to 64%) and its metabolites, 3-MT (to 43%) and HVA (to 68% of controls) **(Table 2).** However, the content of DOPAC was not changed, resulting in a significant increase in DOPAC/DA ratio (138% versus control, **Table 3).** The very low levels of 3-MT **(**Brown *et al.,* 1991; Wood and Altar, 1988**)** in striatum from Aralar-deficient mice and the increase in the ratio of the MAO-derived DA metabolite, DOPAC, over the catechol-*ortho*-methyl-transferase (COMT)-derived DA metabolites, 3-MT and HVA, in Aralar-KO striatum (DOPAC/HVA, 1.38-fold of WT and DOPAC/ 3-MT, 2.35-fold of WT; **Table 3)** suggest an impairment in DA release in these animals. As DOPAC formation requires the intraneuronal MAO–aldehyde dehydrogenase pathway, whereas 3-MT and HVA are formed thanks to COMT in postsynaptic neurons or astrocytes (**see Fig. 6C**), these results also suggests an increase in intraneuronal metabolism of DA in Aralar-KO mice.

Aralar-KO limbic system shows an important reduction in DA (57%) and DOPAC (50%); but only a slight decrease in HVA **(Table 1).** It is unlikely that DA release is particularly diminished in the limbic system, even though 3-MT levels are reduced (**Table 2**), the HVA/DA ratio, which reflects DA turnover via COMT, which functions on

the released DA (Rivett *et al*., 1983), is increased (**Table 3**). In addition, the drop in DA content in the limbic system of Aralar-KO mice does not appear to be due to increased in intracellular metabolism of DA (DOPAC/DA ratio) **(Table 3).**

In conclusion, the Aralar-KO mouse brain shows no changes in NA but a significant decrease in serotonin only in diencephalon and brainstem, brain regions rich in 5HT neurons. As for the DA system, although DA and metabolites did not change in brain regions rich in DA somata, i.e. diencephalon and brainstem, marked decreases in DA were found in areas enriched in DAergic nerve terminals. These results (**summarized in Fig. 6A**) suggest a clear decrease in DA release and increase in DA intracellular metabolism in striatum, but no obvious changes in turnover or release in the limbic system.

DA markers of presynaptic and postsynaptic terminals in striatum and limbic system

A further analysis for DA markers in striatum and limbic system, is shown in **Fig 6D-F**. Remarkably, there is a significant reduction of the DAergic markers VMAT2, the presynaptic vesicular transporter of monoamines, and DARPP32, the dopamine and cAMP regulated phosphoprotein of 32 kDa present in striatal postsynaptic medium spiny neurons (Fienberg *et al*., 1998) in striatum (**Fig. 6E**), but not in the limbic system (**Fig 6F**) of Aralar-KO mice. However, no changes in TH and the dopamine transporter DAT were found in striatum from Aralar-KO mice indicating no gross modifications in the density of presynaptic DAergic terminals. The content of GFAP and OX6 as gliosis markers was unchanged in Aralar-deficient striatum compared to controls (**not shown**).

DARPP32 is mainly expressed in mature medium spiny neurons which are GABAergic (Fienberg *et al.*, 1998). We have previously noted a 40% decrease in striatal GABA levels in Aralar-KO mice (**Table 1**). However, the remarkable lack of postsynaptic DARPP32 in striatum from Aralar-deficient mice (**Fig. 6E**) was not accompanied by any change in the GABA synthesis enzyme GAD, a more immature marker for GABA-containing neurons (**not shown**). These results suggest a deficiency in maturation of medium spiny GABA neurons in aralar-deficient striatum.

Regarding presynaptic DA terminals, the fall in VMAT2 (of about 42%) suggests that the vesicular storage of DA is also impaired in aralar-deficient striatum.

Increased oxidative stress in aralar-KO striatum

The increase in the DOPAC/DA ratio in Aralar-KO striatum **(Table 3**) indicates an increased intracellular oxidation of DA which would lead to an increase of H_2O_2 formation via mitochondrial MAO activity (**Fig. 7**) which could result in a selective oxidative stress in DAergic neurons (Spina and Cohen, 1989). To verify this hypothesis, we measured the content of reduced (GSH) and oxidized glutathione (GSSG) in striatum and other brain regions (limbic system and brainstem) as readout of the cellular redox state (White *et al.*, 1986; Spina and Cohen, 1989).

No changes in GSH levels were found in striatum but the content of GSSG was more than two-fold higher in Aralar-KO compared to WT mice (**Fig. 6B**). GSH and GSSG content in Aralar-KO mice was unchanged in the other brain regions analyzed (limbic system and brainstem; **Fig. S2**). The decreased GSH/GSSG ratio in Aralar-deficient striatum, suggests that this brain region is subjected to high oxidative stress (**Fig. 6B**).

DISCUSSION

Aralar-KO mice present a short lifespan, dying at PND20-22, with generalized tremor and motor coordination defects (Jalil *et al*., 2005). Now we show that Aralar-KO mice exhibit a marked retardation in neurodevelopment, hyper-reactivity, hyper-activity, anxiety, motor discoordination and lack of postural control. CNS from Aralar-KO mice have no apparent neuronal cell death but show a severe hypomyelination and modifications in cortical projections (Jalil *et al*., 2005; Sakurai *et al*., 2010; Ramos *et al*., 2011). In fact, KO mice showed a pronounced shutdown in the major myelin lipids galactocerebrosides, myelin proteins, (Jalil *et al*, 2005) and in mRNAs encoding for proteins involved in myelination (**Table S1**). However, the severity of the phenotype observed in Aralar-KO mice cannot be explained exclusively by hypomyelination as hypomyelination and even the absence of CNS myelin has been proved not to be lethal *per se* in mice (Wolf *et al*., 1999; Matalon *et al*., 2000).

Aralar-KO mice show a higher exploratory activity, hyperactivity and anxious-like behaviour with aversive conditions as well as an increase in rearing; parameters that are known to be sensitive to interferences with the DAergic system (Bernardi *et al*., 1981). Herein, we also observe that Aralar-KO mice have a loss in motor coordination and alterations in the gait pattern and equilibrium, deficits that have been extensively associated to striatal DAergic damage (Menéndez *et al*., 2006; Taylor *et al*., 2011). Failure to perform homing test, in Aralar-KO mice, constitutes a reliable indicator of reduced motivation associated to dopamine deficiency (Palmiter, 2008), but deficits in olfactory discrimination is one of the first nonmotor symptoms observed in patients with Parkinson and in a mice model for DAergic damage (Taylor *et al*., 2011). Accordingly to the behavior observations, KO mice (PND20) showed depletion of DA in DA projection-rich areas, striatum and limbic system, and DA turnover was found to be

highly increased in striatum. Significant increased DA turnover was also observed in striatum of adult (18 months-old) and healthy Aralar-hemizygote mice (Llorente-Folch *et al.*, unpublished). The KO mice also showed a marked decrease in 5-HT and its metabolite 5-HIAA in brainstem and diencephalon, the regions with higher 5-HT levels in control animals. An increase in locomotion and DA turnover could be associated to acceleration of cellular DA uptake (Husain *et al.*, 1994), as supported by the higher DAT/VMAT2 ratio found in Aralar-KO striatum as compared to controls. However, hyperactivity in open field might be also related to anxiety-dependent behavior, due to DA (Zweifel *et al.*, 2011) and 5HT depletions (for review, Fernandez and Gaspar, 2011), since it was only detected in novelty-related experimental situations.

Nigrostriatal DAergic system and striatum, seem to be preferentially vulnerable to Aralar-MAS deficiency in agreement with the notion that striatum is highly susceptible to mitochondrial dysfunctions (Pickrell *et al.*, 2011). We report a marked enlargement in the lateral ventricles with a significant decrease in the size of striatum of Aralar-KO mice. This reduction in size might be related to an extensive lack of myelin and/or to a loss of neuronal projections in this region (Ramos *et al.*, 2011). Together with these findings, fall in GABA (striatum was the only brain region presenting a significant shutdown) and a pronounced decline in Glutamate and Glutamine were found. Our results now reveal two new defects related to Aralar deficiency in striatum: 1) Inability of GABAergic striatal neurons to achieve a mature phenotype. These neurons remain immature as reflected by the spared DARPP32 (a protein that mediates DAergic neurotransmission in almost all the medium spiny neurons), with little variations in GABA or GAD expression; and, 2) loss of DA and DA mishandling reflected by increased DOPAC/DA ratio. The significant reduction in striatal VMAT2 of Aralar- KO mice supports that the presynaptic DAergic nerve endings are damaged but still present

since DAergic markers as TH and DAT were unaffected. In contrast to striatum, in regions enriched in DAergic somata as brainstem and diencephalon, DA content was found to be increased, perhaps due to an attempt to compensate for any dysfunction in the surviving DAergic neurons, as occurrs in the very early stages of Parkinson´s disease (PD) (Hefti *et al*., 1980; Hornykiewicz and Kish, 1987; Altar *et al*., 1987).

The impairment of the dopaminergic system, particularly in the dopaminergic striatal terminals of the Aralar-KO mouse, is probably related, besides to its specific vulnerability to oxidative stress, to an increase in oxidative stress caused by the lack of Aralar-MAS activity. This increased oxidative stress was reflected, between others, in the very significant decrease in the GSH/GSSG specifically in Aralar-KO striatum. Although total GSH, the most abundant antioxidant in brain found to be decreased in DAergic pathology as PD (Sofic *et al*., 1992; Pearce *et al*., 1997; Pisani *et al*., 2006), was not significantly changed. In Aralar-KO mice, striatal GSSG, representing aprox. 1% of the total glutathione, was more than two-fold of control value. Because GSSG increase was probably localized mainly to DA nerve terminals which constitute only 1% or less of the mass of the striatum; this signify very much higher concentrations of GSSG within DA terminals of Aralar-KO striatum. The very significant decrease in the GSH/GSSG specifically in Aralar-KO striatum is related to increased oxidative stress (Spina and Cohen, 1981) in the cytosol which has the largest GSH pool and/or the mitochondria that contains a much smaller GSH pool (Murphy, 2011). Although we believe that the initial decrease in GSH is mitochondrial (see below), H_2O_2 escaped from mitochondria to the cytosol probably contributes to the decrease in cytosolic GSH/GSSG.

Mitochondria produce O_2^- and H_2O_2 which are detoxified by thanks to GSH and thioredoxin together with a number of enzymes that ultimately use one of these two thiol molecules as redox agents (Murphy, 2011), The regeneration of the reduced

forms of glutathione and thioredoxin requires NADPH. There are three systems which produce NADPH in brain mitochondria, NADP-isocitrate dehydrogenase, malic enzyme and energy dependent nicotinamide nucleotide transhydrogenase (NNT) (Andres *et al*. 1980; Albracht *et al*., 2011). The third of these systems, NNT, utilyzes mitochondrial NADH and the proton electrochemical gradient to produce NADPH. There is evidence that NNT is important in supplying NADPH for mitochondrial detoxification, as the lack of NNT increased O_2-/H_2O_2 production in mitochondria of beta cells (Freeman *et al*., 2006).

NADPH production through NNT may be limited by mitochondrial NADH production. In brain, which utilizes glucose as main energy source, mitochondria produce NADH from pyruvate in the tricarboxylic acid cycle. The lack of Aralar results in a pronounced decrease in MAS, the major NADH shuttle in brain, (Jalil *et al*., 2005) resulting in an increased lactate-to-pyruvate ratio (Pardo *et al*., 2011), and in a limitation in pyruvate supply to mitochondria as reflected in a reduced maximal respiration rate in intact neurons (Gómez-Galán *et al*., 2011). This scenario is one in which mitochondrial NADH production is clearly limited, and this will result in a lack of inactivation of O_2^- and H_2O_2 which will cause oxidative damage to Aralar-KO mitochondria, and the escape of H_2O_2 to the cytosol (Han *et al*., 2003), causing oxidative stress in this cellular compartment.

ROS formation is further potentiated in Aralar-KO striatum because VMAT2 deficiency resulting in an increase in non-vesicular DA that might favour both MAO-mediated oxidation and autooxidation of non-protected cytosolic DA. These two processes lead to the formation of ROS such as hydrogen peroxide, and reactive quinone and semi-quinone species produced by DA autooxidation (Graham, 1978; Maker *et al*., 1981). Furthermore, DACHR (*o*-quinone dopaminochrome, a product of DA oxidation)

has been reported to increase, in a dose-dependent way, the production of H_2O_2 constitutively observed at Complex I of the mitochondrial respiratory chain (Zoccarato *et al.*, 2005). Our data suggest that the rate of production of ROS evoked by Aralar deficiency in striatum override cellular mechanisms for reducing GSSG and might have important consequences in the DA neuronal physiology that are more sensitive to oxidative stress (Drechsel and Patel, 2008; Zeevalk *et al.*, 1997). Besides enhanced ROS formation, DA neurons are prone to ROS attack, i.e. the scarce proportion of glial cells surrounding DA neurons in the substantia nigra (for review, Mena *et al.*, 2002), the presence of neuromelanin pigment in subpopulations of DA-containing mesencephalic neurons (Hirsch *et al.*, 1988) and the low content of mitochondria in DA neurons of the substantia nigra pars compacta (Liang *et al.*, 2007) might be mentioned between other characteristics.

Decreased VMAT2 expression was found exclusively in striatum, but not in limbic system, of Aralar-KO mice as a remarkable event involved in DAergic neurodegeneration. This fact was previously reported as a key pathogenic event preceding nigrostriatal dopamine neurodegeneration and clinical manifestations in a primate model of PD (Chen *et al.*, 2008). These authors suggested that loss of VMAT2 might be due to an association with α-synuclein aggregates induced by oxidative stress as a result of (1-methyl-4-phenyl-1,2,3,6-tetrahydropiridine) MPTP, a DA toxin, treatment. Accordingly to this, previous work had proposed a direct interaction between VMAT2 and α-synuclein, disrupting synaptic vesicle dynamics (Lotharius and Brundin, 2002; Mosharov *et al.*, 2006; Guo *et al.*, 2008; for references, Taylor *et al.*, 2011). Consequently, in the Aralar-KO mice, the marked decrease in mitochondrial NADH and ROS detoxyfication capacity might result in oxidative stress (**see Fig. 7**); but, if VMAT2 loss is related to its sequestration with alpha-synuclein aggregates remains an open

question in our model. The mishandling of DA via reduced VMAT2, associated to an increased striatal DOPAC/DA (**Fig. 6A)**, and GSSG/GSH ratios (**Fig. 6B**), might be sufficient to cause DA-mediated toxicity and neurodegeneration in the nigrostriatal DA system (Mooslehner *et al*., 2001; Caudle *et al*., 2007; for review, see Taylor *et al*., 2011). These data point out the close relationship between Aralar-MAS activity and DA handling in the nigrostriatal pathway.

Besides the decrease in VMAT2 content, decrease in VMAT2 activity by nitration might be another possible mechanism involved in ROS attack (Guo *et al*., 2008; Watabe and Nakabi, 2008). It is worth also to note that the presence of VMAT2 in presynaptic vesicles attenuates the deleterious effect of MPTP, the most powerful toxin for dopaminergic neurons linked to the genesis of PD. Indeed, in VMAT2 heterozygous knockout mice, MPTP toxicity was twice that observed in wild-type mice (Gainetdinov *et al*., 1998); and a selective reduction in dopamine storage by VMAT2 might be a pathogenic feature of PD (Lee *et al*., 2000).

The present results demonstrate that AGC1-MAS deficiency in mice might be considered as a CNS disorder targeting monoaminergic brain systems specifically striatum, with no apparent pathology in muscle, where Aralar is also highly expressed. DA neurotransmission is also altered in mice with mutations of α- synuclein, parkin or DJ-1, considered as suitable models for PD studies. These mice, similar to what is reported herein for Aralar-KO and previously for VMAT2-KO mice (Colebrooke *et al*., 2006), do not display loss of midbrain DA neurons, the hallmark of Parkinson's disease (Dawson *et al*., 2010, for references). It is worth to take into account that mice possess low neuromelanin and high GSH content what might render them specially resistant to DA degeneration compared to primates and humans. These factors would contribute to underestimate the detrimental effects of Aralar-MAS deficiency on the DA system in

humans. Deficiencies or failure in the operation of the Aralar-MAS pathway, resulting in a limited mitochondrial NADH formation and ROS detoxyfing capacity, might constitute an important factor at the origin of DA degeneration and its implication in human pathologies as Parkinson´s and Huntington´s diseases might be thoughtfully explored. Novel therapeutics in human to optimize Aralar-MAS shuttle function in brain might improve healthy physiology of DA neurons and/or prevent them from degeneration.

ACKNOWLEDGEMENTS

This work was supported by grants from the Ministerio de Educación y Ciencia BFU2008-04084/BMC (to JS), and Ciencia e Innovación (SAF2010-16427 to MD), Comunidad de Madrid S-GEN-0269-2006 MITOLAB-CM (to JS), European Union Grant LSHM-CT-2006-518153 (to J.S.), and CureFXS E-Rare. EU/FIS PS09102673, Spanish Ministry of Health (PI 082038 to MD), Marató TV3, Jerome Lejeune (JMLM/AC/08-044) to MD, Fundación Médica Mutua Madrileña (to BP), and by an institutional grant from the Fundación Ramón Areces to the CBMSO. CIBERER is an initiative of the ISCIII.

The authors thank to Isabel Manso, Barbara Sesé and Dolores Cano for technical support. IL-F is a recipient of a predoctoral contract from the Comunidad de Madrid, Spain.

Conflict of Interest statement. None declared

REFERENCES:

Albracht S.P., Meijer A.J., Rydström J. (2011) Mammalian NADH:ubiquinone oxidoreductase (Complex I) and nicotinamide nucleotide transhydrogenase (Nnt)

together regulate the mitochondrial production of H_2O_2-Implications for their role in disease, especially cancer. *J. Bioenerg. Biomembr.* **43**, 541–564.

Altar C.A., Marien M.R. and Marshall J.F. (1987) Time course of adaptations in dopamine biosynthesis, metabolism, and release following nigrostriatal lesions: implications for behavioral recovery from brain injury. *J. Neurochem.* **48**, 390-399.

Altman J. and Sudarshan K. (1975) Postnatal development of locomotion in the laboratory rat. *Anim. Behav.* **23**, 896-920.

Andres A., Satrústegui J. and Machado A. (1980) Development of NADPH producing pathways in rat heart. *Biochem. J.* **186**, 799-803.

Bernardi M.M., De Souza H. and Palermo Neto J. (1981) Effects of single and long-term haloperidol administration on open field behavior of rats. *Psychopharmacol.* **73**, 171-175.

Berkich D.A., Ola M.S., Cole J., Sweatt A.J., Hutson S.M. and LaNoue K.F. (2007) Mitochondrial transport proteins of the brain. *J. Neurosci. Res.* **85**, 3367–77.

Brown E.E., Damsma G., Cumming P. and Fibiger H.C. (1991) Intersticial 3-methoxytyramine reflects striatal dopamine release: an in vivo microdialysis study. *J. Neurochem.* **57**, 701-707.

Cahoy J.D., Emery B., Kaushal A. *et al*. (2008) A transcriptome database for astrocytes, neurons, and oligodendrocytes: a new resource for understanding brain development and function. *J. Neurosci*. **28**, 264–278.

Canals S., Casarejos M.J., Rodriguez-Martin E., de Bernardo S.and Mena M.A. (2001) Neurotrophic and neurotoxic effects of nitric oxide on fetal midbrain cultures. *J. Neurochem.* **76**, 56-68.

Carlsson A. and Lindqvist M. (1973) Effect of ethanol on the hydroxylation of tyrosine and tryptophan in rat brain in vivo. *J. Pharm. Pharmac.* **25**, 437-440.

Carola V., DÓlimpio F., Brunamonti E., Mangia F. and Renzi P. (2002) Evaluation of the elevated plus-maze and open-field tests for the assessment of anxiety-related behavior in inbred mice. *Behav. Brain Res*. **144**, 49-57.

Caudle W.M., Richardson J.R., Shepherd K.R., Taylor T.N., Guillot T.S., McCormack A.L., Colebrooke R.E., Di Monte D.A., Emson P.C. and Miller G.W. (2007) Reduced vesicular storage of dopamine causes progressive nigrostriatal neurodegeneration. *J. Neurosci.* **27**, 8138-8148.

Colebrooke R.E., Humby T., Lynch P.J., McGowan D.P., Xia J.and Emson P.C. (2006) Age-related decline in striatal dopamine content and motor performance occurs in the absence of nigral cell loss in a genetic mouse model of Parkinson´s disease. *Eur. J. Neurosci.* **24**, 2622-2630.

Contreras L., Urbieta A., Kobayashi K., Saheki T. and Satrústegui J. (2010) Low levels of citrin (SLC25A13) expression in adult mouse brain restricted to neuronal clusters. *J. Neurosci. Res*. **88**, 1009–1016.

Chen M.K., Kuwabara H., Zhou Y. *et al*. (2008) VMAT2 and dopamine neuron loss in a primate model of Parkinson´s disease. *J. Neurochem*. **105**, 78-90.

Dawson T.M., Ko H.S. and Dawson V.L. (2010) Genetic animal models of Parkinson´s disease. *Neuron* **66**, 646-661.

Del Arco A. and Satrústegui J. (1998) Molecular cloning of aralar, a new member of the mitochodrial carrier superfamily that binds calcium and is present in human muscle and brain. *J. Biol. Chem*. **273**, 23327-23334.

Dierssen M., Fotaki V., Martínez de Lagrán M., Gratacos M., Arbones M., Fillat C. and Estivill X. (2002) Neurobehavioural development of two mouse lines commonly used in transgenic studies. *Pharmacol. Biochem. Behav*. **73**, 19-25.

Drechsel D.A and Patel M. (2008) Role of reactive oxygen species in the neurotoxicity of environmental agents implicated in Parlkinson´s disease. *Free Radic Biol Med* **44**, 1873-1886.

Fernandez S.P. and Gaspar P. (2011) Investigating anxiety and depressive-like phenotypes in genetic mouse models of serotonin depletion. *Neuropharmacol.* **62**, 144-54.

Fienberg A.A., Hiroi N., Mermelstein P.G. *et al.* (1998) DARPP-32: Regulator of the efficacy of dopaminergic neurotransmission. *Science* **281**, 838-842.

Freeman H., Shimomura K., Horner E., Cox R.D. and Ashcroft F.M. (2006) Nicotinamide nucleotide transhydrogenase: a key role in insulin secretion. *Cell Metab.* **3**, 35-45.

Gainetdinov R.R., Fumagalli F., Wang Y.M., Jones S.R., Levey A.I., Miller G.W. and Caron M.G. (1998) Increased MPTP neurotoxicity in vesicular monoamine transporter 2 heterozygote knockout mice. *J. Neurochem*. **70**, 1973-1978.

Gómez-Galán M., Makarova J., Llorente-Folch I., Saheki T., Pardo B., Satrústegui J.and Herreras O. (2012) Altered postnatal development of cortico-hippocampal neuronal electric activity in mice deficient for the mitochondrial aspartate-glutamate transporter. *J. Cereb. Blood Flow Metab* **32**, 306-317.

Graham .DG. (1978) Oxidative pathways for catecholamines in the genesis of neuromelanin and cytotoxic quinones. *Mol. Pharmacol.* **14**, 633–643.

Guo J.T., Chen A.N.Q., Kong Q.I., Zhu H., Ma C.M. and Qin C. (2008) Inhibition of vesicular monoamine transporter-2 activity in α-synuclein stably transfected SH-SY5Y cells. *Cell. Mol. Neurobiol*. **28**, 35-47.

Han D., Antunes F., Canali R., Rettori D. and Cadenas E. (2003) Voltage-dependent anion channels control the release of the superoxide anion from mitochondria to cytosol. *J. Biol. Chem*. **278**, 5557-5563.

Hauber W. (1998) Involvement of basal ganglia transmitter system in movement initiation. *Prog. Neurobiol*. **56**, 507-540.

Hefti F., Melamed E. and Wurtman R.J. (1980) Partial lesions of the dopaminergic nigrostriatal system in rat brain: biochemical characterization. *Brain Res*. **195**, 123-137.

Hirsch E., Graybiel A.M.and Agid Y.A. (1988) Melanized dopaminergic neurons are diferentially susceptible to degeneration in Parkinson´s disease. *Nature* **334**, 345-348.

Hornykiewicz O. and Kish S.J. (1987) Biochemical pathophysiology of Parkinson´s disease. *Adv. Neurol*. **45**, 19-34.

Husain R., Malaviya M., Seth P.K.and Husain R. (1994) Effect of deltamethrin on regional brain polyamines and behaviour in young rats. *Pharmacol. Toxicol*. **74**, 211-215.

Itier J.-M., Ibañez P., Mena M.A. *et al*. (2003) Parkin gene inactivation alters behaviour and dopamine neurotransmission in the mouse. *Hum. Mol. Genet*. **12**, 2277-2291.

Jalil M.A., Begum L., Contreras L. *et al*. (2005) Reduced N- acetylaspartate levels in mice lacking Aralar, a brain- and muscle-type mitochondrial aspartate-glutamate carrier" *J. Biol. Chem.* **280**, 31333-31339.

Lee C.S., Samii A., Sossi V. *et al*. (2000) In vivo positron emission tomographic evidence for compensatory changes in presynaptic dopaminergic nerve terminals in Parkinson´s disease. *Ann. Neurol*. **47**, 493-503.

Lepagnol-Bestel A.-M., Maussion G., Boda B. *et al*. (2008) SLC25A12 expression is associated with neurite outgrowth and is upregulated in the prefrontal cortex of autistic subjects. *Mol Psychiatry*. **13**, 385-397.

Liang Ch. L., Wang T.T., Luby-Phelps K. and German D.C. (2007) Mitochondria mass is low in mouse substantia nigra dopamine neurons: Implications for Parkinson´s disease. *Exp. Neurol*. **203**, 370-380.

Lotharius J. and Brundin P. (2002) Pathogenesis of Parkinson´s disease: dopamine, vesicles and alpha-synuclein. *Nature Rev. Neurosci*. **3**, 932-942.

Maker H.S., Weiss C., Silides D.J. and Cohen G. (1981) Couple of dopamine oxidation monoamine oxidation via the generation of hydrogen peroxide in rat brain homogenates. *J. Neurochem*. **36**, 589-593.

Matalon R., Rady P.L., Platt K.A. *et al*. (2000) Knock-out mouse for Canavan disease: a model for gene transfer to the central nervous system. *J. Gene Med*. **2**, 165-175.

Mena M.A., Pardo B., Paino C.L. and De Yébenes J.G. (1993) Levodopa toxicity in foetal rat midbrain neurones in culture: modulation by ascorbic acid. *Neuroreport* **4**, 438-440.

Mena M.A., Garcia de Yébenes M.J., Tabernero C., Casarejos M.J., Pardo B. and Garcia de Yébenes J. (1995) Effects of calcium antagonists on the dopamine system. *Clin. Neuropharmacol.* **18**, 410-426.

Mena M.A., Khan U., Togasaki D.M., Sulzer D., Epstein C.J. and Przedborski S. (1997) Effects of wild-type and mutated copper/zinc superoxide dismutase on

neuronal survival and L-DOPA-induced toxicity in postnatal midbrain culture. *J. Neurochem.* **69**, 21-33.

Mena M.A., de Bernardo S., Casarejos M.J., Canals S. and Rodríguez-Martin E. (2002) The role of astroglia on the survival of dopamine neurons. *Mol. Neurobiol.* **25**, 245-263.

Menéndez J., Rodríguez-Navarro J.A., Solano R.M., Casarejos M.J., Rodal I., Guerrero R., Sánchez M.P., Avila J., Mena M.A. and de Yébenes J.G. (2006) Supression of parkin enhances nigrostriatal and motor neuron lesion in mice over-expressing human-mutated tau protein. *Hum. Mol. Genet.* **15**, 2045-2058.

Mooslehner K.A., Chan P.M., Xu W., Liu L., Smadja C., Humby T., Allen N.D., Wilkinson L.S.and Emson P.C. (2001) Mice with very low expression of the vesicular monoamine transporter 2 gene survive into adulthood: potential mouse model for parkinsonism. *Mol. Cell Biol.* **21**, 5321-5331.

Mosharov E.V., Staal R.G.W., Bové J. *et al.* (2006) α-synuclein overexpression increases cytosolic catecholamine concentration. *J. Neurosci.* **26**, 9304-9311.

Murphy M.P. (2012) Mitochondrial thiols in antioxidant protection and redox signalling: distinct roles for glutathionylation and other thiol modifications. *Antioxidants & Redox Signaling* **16**, 476-495.

Palmieri L., Papaleo V., Porcelli V., *et al.* (2008) Altered calcium homeostasis in autism-spectrum disorder: Evidence from biochemical and genetic studies of the mitochondrial aspartate/glutamate carrier AGC1. *Mol. Psychiatry* **15**, 38-52.

Palmiter R.D. (2008) Dopamine signaling in the dorsal striatum is essential for motivated behaviors. Lessons for dopamine-deficient mice. *Ann N Y Acad Sci* **1129**, 35-46.

Pardo B., Mena M.A., Casarejos M.J., Paino C.L. and de Yébenes J.G. (1995) Toxic effects of L-DOPA on mesencephalic cell cultures: protection with antioxidants. Brain Res. **682**, 133-143.

Pardo B., Contreras L., Serrano A., Ramos M., Kobayashi K., Iijima M., Saheki T. and Satrústegui J. (2006) Essential role of aralar in the transduction of small calcium signals to neuronal mitochondria *J. Biol. Chem*. **281**, 1039-1047.

Pardo B., Rodrigues T.B., Contreras L., Garzón M., Llorente-Folch I., Kobayashi K., Saheki T., Cerdán S. and Satrústegui J. (2011) Brain glutamine synthesis requires neuronal-born aspartate as amino donor for glial glutamate formation. *J. Cereb. Blood Flow Metab.* **31,** 90-101.

Pearce R.K., Owen A., Daniel S., Jenner P. and Marsden C.D. (1997) Alterations in the distribution of glutathione in the substantia nigra in Parkinson's disease. *J. Neural Trans.* **104**, 661-677.

Pickrell A.M., Fukui H., Wang X., Pinto M. and Moraes C. (2011) The striatum is highly susceptible to mitochondrial oxidative phosphorylation dysfunctions. *J. Neurosci*. **31**, 9895-9904.

Pisani A., Martella G., Tscherter A., Costa C., Mercuri N.B., Bernardi G., Shen J. and Calabresi P. (2006) Enhanced sensitivity of DJ-1-deficient dopaminergic neurons to energy metabolism impairment: role of Na+/K+ ATPase. *Neurobiol. Dis*. **23**, 54-60.

Ramos M., del Arco A., Pardo B., *et al*. (2003) Developmental changes in the Ca^{2+}-regulated mitochondrial aspartate-glutamate carrier aralar1 in brain and prominent expression in the spinal cord. *Dev. Brain Res*. **143**, 33-46.

Ramos M., Pardo B., Llorente-Folch I., del Arco A. and Satrústegui J. (2011) The deficiency in the mitochondrial transporter of aspartate/glutamate Aralar/AGC1 causes hypomyelination and neuronal defects unrelated to myelin deficits in mouse brain. *J. Neurosci. Res*. **89**, 2008-2017.

Ramoz N., Reichert J.G., Smith C.J., Silverman J.M., Bespalova I.N., Davis K.L. and Buxbaum J.D. (2004) Linkage and association of the mitochondrial aspartate/glutamate carrier SLC25A12 gene with autism. *Am. J. Psychiatry* **161**, 662-669.

Rivett A.J., Francis A. and Roth, J.A. (1983) Distinct cellular localization of membrane-bound and soluble forms of cathecol-O-methyltransferase in brain. *J. Neurochem*. **40**, 215-219.

Sakurai T., Ramoz N., Barreto M., *et al.* (2010) Slc25a12 disruption alters myelination and neurofilaments: a model for a hypomyelination syndrome and childhood neurodevelopmental disorders. *Biol. Psychiatry* **67**, 887-894.

Segurado R., Conroy J., Meally E., Fitzgerald M., Gill M. and Gallagher L. (2005) Confirmation of association between autism and the mitochondrial aspartate/glutamate carrier SLC25A12 gene on chromosome 2q31. *Am. J. Psychiatry* **162**, 2182-2184.

Smith P.F., Horii A., Russell N., Bilkey D.K., Zheng Y., Lui P., Kerr D.S. and Darlington, C.L. (2005) The effects of vestibular lesions in hippocampal function in rats. *Prog. Neurobiol*. **75**, 391-405.

Sofic E., Lange K.W, Jellinger K. and Riederer P. (1992) Reduced and oxidized glutathione in the substantia nigra of patients with Parkinson´s disease. *Neurosci. Lett.* **142**, 128-130.

Spina M.B. and Cohen G. (1989) Dopamine turnover and glutathione oxidation: implications for Parkinson´s disease. *Proc. Natl. Acad. Sci. USA* **88**,1398-1400.

Stein J.M., Bergman W., Fang Y., Davison L., Brensinger C., Robinson M.B., Hecht N.B. and Abel T. (2006) Behavioral and neurochemical alterations in mice lacking tha RNA-binding protein translin. *J. Neurosci*. **26**, 2184-2196.

Taylor T.N., Caudle W.M. and Miller G.W. (2011) VMAT2-deficient mice display nigral and extranigral pathology and motor and nonmotor symptoms of Parkinson´s disease. Parkinson´s disease 2011; doi: 10.4061/2011/124165.

Turunen J.A., Rehnström K., Kilpinen H., Kuokkanen M., Kempas E.and Ylisaukko-Ojaa, T. (2008) Mitochondrial aspartate/glutamate carrier SLC25A12 gene is associated with autism. *Autism Res*. **1**, 189-192.

Watabe M.and Nakaki T. (2008) Mitochondrial complex I inhibitor rotenone inhibits and redistributes vesicular monoamine transporter 2 via nitration in human dopaminergic SH-SY5Y cells. *Mol. Pharmacol*. **74**, 933-940.

White C.W., Mimmack R.F.and Repine J.E. (1986) Accumulation of lung tissue oxidized glutathione (GSSG) as a marker of oxidant induced lung injury. *Chest (Suppl.)* **89**, 111-113.

Wibom R., Lasorsa F.M., Töhönen V.*et al*., (2009) AGC1 deficiency associated with global cerebral hypomyelination. *New Engl. J. Med.* **361**, 489-495.

Wolf M.K., Nunnari J.N. and Billings-Gagliardi S. (1999) Quaking shiverer double-mutant mice survive for at least 100 days with no CNS myelin. *Dev. Neurosci*. **21**, 483-490.

Wood P.L. and Altar C.A. (1988) Dopamine release in vivo from nigrostriatal, mesolimbic and mesocortical neurons: utility of 3-methoxytyramine measurements. *Pharmacol. Rev.* **40**, 163-187.

Xu Y., Ola M.S., Berkich D.A. *et al*. (2007) Energy sources for glutamate neurotransmission in the retina: absence of the aspartate/glutamate carrier produces reliance on glycolysis in glia. J. Neurochem. **101**, 120-131.

Zeevalk G.D., Manzino L., Hoppe J. and Sonsalla P. (1997) In vivo vulnerability of dopamine neurons to inhibition of energy metabolism. *Eur. J Pharmacol*. **320**, 111-119.

Zoccarato F., Toscano P. and Alexandre A. (2005) Dopamine-derived dopaminochrome promotes H_2O_2 release at mitochondrial complex I. *J. Biol. Chem*. **280**, 15587-15594.

Zweifel L.S., Fadok J.P., Argilli E. *et al*. (2011) Activation of dopamine neurons is critical for aversive conditioning and prevention of generalized anxiety. *Nature Neurosci*. **14**, 620-626.

Table 1. Amino acid content in brain extracts from Aralar WT and Aralar KO mice at 20 days (striatum, diencephalon, hipocampus, brain stem, cerebral cortex, and cerebellum).

Aminoacids (nmol/g tissue)		**Striatum**	**Diencephalon**	**Limbic system**	**Brain stem**	**Cer. Cortex**	**Cerebellum**
Aspartate	Aralar WT	2264 ± 175	2466 ± 122	1894 ± 232	2409 ± 156	2356 ± 91	2379 ± 62
	Aralar KO	454 ± 41 ***	429 ± 21 ***	399 ± 48 **	562 ± 34 ***	430 ± 54 ***	706 ± 61 ***
	(% vs WT)	**20%**	**17%**	**21%**	**23%**	**18%**	**29%**
Serine	Aralar WT	1101 ± 90	790 ± 74	1014 ± 159	514 ± 19	1000 ± 33	709 ± 48
	Aralar KO	160 ± 16 ***	164 ± 13 **	138 ± 9 **	168 ± 26 ***	196 ± 24 ***	215 ± 18 **
	(% vs WT)	**14%**	**21%**	**13.6%**	**33%**	**20%**	**30%**
Alanine	Aralar WT	783 ± 97	573 ± 39	870 ± 128	525 ± 18	805 ± 22	497 ± 19
	Aralar KO	297 ± 63 **	180 ± 18 ***	211 ± 15 **	238 ± 36 ***	261 ± 23 ***	201 ± 19 ***
	(% vs WT)	**38%**	**31%**	**24%**	**45%**	**32%**	**40%**
Glutamate	Aralar WT	7512 ± 487	7615 ± 321	8166 ± 1076	5840 ± 258	8326 ± 252	8071 ± 237
	Aralar KO	4030 ± 238 **	3935 ± 230 ***	4446 ± 577 **	4141 ± 235 **	5797 ± 575 **	5202 ± 418 ***
	(% vs WT)	**54%**	**52%**	**54.4%**	**71%**	**70%**	**64%**
Glutamine	Aralar WT	3019 ± 258	2880 ± 143	2548 ± 301	2653 ± 205	2449 ± 231	3808 ± 143
	Aralar KO	895 ± 166 ***	1387 ± 233 **	1133 ± 268 **	2569 ± 185	1471 ± 264 **	3119 ± 352 *
	(% vs WT)	**29%**	**48%**	**44.4%**	**97%**	**60%**	**82%**
GABA	Aralar WT	2523 ± 260	2563 ± 237	1568 ± 221	1543 ± 133	1558 ± 68	1442 ± 103
	Aralar KO	1512 ± 141 **	2682 ± 116	1223 ± 159	1979 ± 194 *	1863 ± 88 **	1062 ± 93
	(% vs WT)	**60%**	**105%**	**77%**	**128%**	**119%**	**74%**

cv

Results are expresssed in nmol per gr of tissue. Values are the mean ± s.e.m. (n=3-6). Statistical analysis was performed by one-way analysis of variance followed by Student-Newman-Keuls t-test. *, $p < 0.05$; **, $p < 0.01$; ***, $p < 0.001$ Aralar KO versus Aralar WT mice.

Table 2- Monoamine metabolism in striatum, diencephalon, limbic system and brainstem of Aralar WT and Aralar KO mice.

Monoamines (nmol/g tissue)		Striatum	Diencephalon	Limbic system	Brain stem
DA	Aralar WT	5690 ± 525	341 ± 92	1412 ± 220	97.7 ± 18
	Aralar KO	3661 ± 175 **	431 ± 88	810 ± 82 *	164 ± 51
	(% vs WT)	**64%**	**126%**	**57%**	**168%**
3-MT	Aralar WT	330 ± 39	n.d ≤ 6	59.7 ± 6.2	n.d ≤ 6
	Aralar KO	142 ± 29 **	n.d ≤ 6	n.d ≤ 6	n.d ≤ 6
	(% vs WT)	**43%**			
DOPAC	Aralar WT	387 ± 10	84 ± 10	141 ± 14	43.8 ± 2.7
	Aralar KO	362 ± 38	127 ± 10 *	71 ± 17 **	73.7 ± 8 **
	(% vs WT)	**93%**	**151%**	**50%**	**168%**
HVA	Aralar WT	681 ± 35	219 ± 21	136.5 ± 12.1	61.6 ± 6.4
	Aralar KO	468 ± 64 *	279 ± 18	115.2 ± 6.6	85.2 ± 7.5 *
	(% vs WT)	**68%**	**127%**	**85%**	**138%**
NA	Aralar WT	251 ± 20	846 ± 22	336 ± 20	1223 ± 60
	Aralar KO	265 ± 30	1008 ± 98	320 ± 28.8	1359 ± 36.5
	(% vs WT)	**105%**	**119%**	**95%**	**111%**
5-HT	Aralar WT	333 ± 67	1501 ± 242	585 ± 55	1988 ± 39
	Aralar KO	250 ± 89	768 ± 88 *	460 ± 58	1445 ± 172 *
	(% vs WT)	**75%**	**51%**	**79%**	**72%**
5-HIAA	Aralar WT	256 ± 102	859 ± 95	337 ± 40	484 ± 16
	Aralar KO	99 ± 28	375 ± 42 ***	218 ± 29.5*	285 ± 25 ***
	(% vs WT)	**38%**	**43%**	**64%**	**59%**

Results are expresssed in nmol per gr of tissue. Values are the mean ± s.e.m. (n=6). Statistical analysis was performed by one-way analysis of variance followed by Student-Newman-Keuls t-test. * $p < 0.05$, ** $p < 0.01$, *** $p < 0.001$ Aralar KO versus Aralar WT mice.

Table 3- Turnover of monoaminergic neurons measured in brain regions (striatum, diencephalon, limbic system and brain stem) of Aralar WT and Aralar KO mice.

Ratios (nmol/g tissue)		Striatum	Diencephalon	Limbic system	Brain stem
DOPAC/DA x 10^2	Aralar WT	7.1 ± 0.7	28.4 ± 3.0	11.7 ± 2.1	50.6 ± 7.0
	Aralar KO	9.9 ± 1.0 *	33.8 ± 5.3	8.7 ± 1.7	55.7 ± 7.8
	(% vs WT)	**138%**	**119%**	**78%**	**110%**
HVA/DA x 10^2	Aralar WT	12.6 ± 1.5	76.2 ± 10.3	11.4 ± 2.0	5.6 ± 10.0
	Aralar KO	12.7 ± 1.5	74.0 ± 10.6	15.3 ± 2.0 *	73.7 ± 6.7
	(% vs WT)	**101%**	**97%**	**134%**	**97%**
DOPAC/HVA x 10^2	Aralar WT	57.7 ± 3.0	38.8 ± 3.1	209.0 ± 15.2	67.6 ± 6.9
	Aralar KO	79.7 ± 4 *	45.6 ± 1.1	131.6 ± 35.2	73.9 ±5.6
	(% vs WT)	**138%**	**117%**	**63%**	**109%**
5HIAA/5HT x 10^2	Aralar WT	75.1 ± 16.8	65.3 ± 14.6	58.0 ± 4.0	24.4 ± 0.9
	Aralar KO	55.8 ± 11.3	49.6 ± 3.2	50.2 ± 6.8	20.8 ± 2.3
	(% vs WT)	**74%**	**76%**	**86%**	**85%**

Values are the mean ± s.e.m. (n=6). Statistical analysis was performed by one-way analysis of variance followed by Student-Newman-Keuls t-test. * $p < 0.05$ Aralar KO versus Aralar WT mice.

Legend to Figures:

Figure 1- Neurobehavioral development is strongly affected in Aralar-KO mice. Toe pinch and reaching response at PND17 (**A**). Quantitation of seizures during postnatal development (**B**). Touch escape (**C**) and homing test (**D**, denoting exploratory, social and motor behaviour) are illustrated in wild-type (open circles or bars), Aralar-hemizygote (grey circles or bars) and Aralar-KO mice (filled circles or bars). Data are expressed as the mean ± s.e.m (n= 8-13 mice per group). .* $p \leq 0.05$, ** $p \leq 0.01$, *** $p \leq 0.001$.

Figure 2- Openfield studies show high levels of hyperactivity and anxiety in Aralar-KO mice. Parameters as total travelled distance (**A**), mean speed of walk (**B**) and resting time between displacements (**C**) in the center and periphery of the arena and at dark (basal)-light (aversive) conditions are valutated in WT, Aralar-hemizygote and Aralar-KO mice. Data are expressed as the mean ± s.e.m (n=8-13 mice per group). * $p \leq 0.05$, ** $p \leq 0.01$.

Figure 3- Aralar-KO mice showed a marked improvement in postural control, delayed neurodevelopment and lack of equilibrium. Surface righting response (**A**), wire suspension (**B**), negative geotaxis (**C**), and latency from pivoting to walking (**D**) were studied at indicated PNDs in wild-type (open circles or bars), Aralar-hemizygote (grey circles or bars) and Aralar-KO mice (filled circles or bars). Data are expressed as the mean ± s.e.m (n = 8-13 mice per group). .* $p \leq 0.05$, ** $p \leq 0.01$, *** $p \leq 0.001$.

Figure 4- Aralar-KO mice have a dramatic motor discoordination. In the pawprinting test (**A, B**) it is noticeable that Aralar-KO mice have a shorter stride length and a shorter hindpaw length than the WT siblings (**A**), and an erratic direction of walk (**B**). Asymetric

gait at the right leg is shown in the footprint left by the hind limbs of Aralar-KO mice walking on the paper (**B**). The beam balance test (**C**) was performed in wild-type (open circles), Aralar-hemizygote (grey circles) and Aralar-KO mice (filled circles). 1 and 2- indicates the number of assay. (n=10-13 mice per group).

Figure 5- Aralar-KO mice show no morphological abnormalities in brain, with an enlargement in lateral ventricule and a reduction in size of striatum as compared to their WT siblings. View of coronal sections are shown stained with cresyl violet in wild-type (wt) and Aralar-KO animals at PND20 (scale bar, 500 μm) (**A**). (**B**) Quantitation of the area for striatum and hippocampus versus that of whole brain is represented, as percentage, in Aralar-WT (open bars) and Aralar-KO mice (filled bars; n= 4). (**C**) View of coronal sections of the brain from WT and Aralar-KO mice at PND20 as observed at the high power (scale bar, 500 μm). Data are expressed as the mean ± s.e.m (n = 6 mice). (**D**) The number of positive-neurons for TH in the substantia nigra (SN) and midbrain was found to be equal in Aralar-KO as compared to control mice. * $p \leq 0.05$.

Figure 6- Striatum appeared to be the most affected region in Aralar-deficient brain. (**A**) Differential effects of Aralar deficiency on DA metabolism in brain regions enriched in DA terminals (striatum and limbic system). DA and its metabolites, except DOPAC, are significantly decreased in Aralar-KO striatum. DA turnover is increased in Aralar-KO striatum. (**B**) The enhanced striatal DA turnover provoked an increase in cellular oxidative stress as measured by GSH/GSSG ratios. (**C**) Scheme of tyrosine metabolism into the presynaptic and postsynaptic neurons in striatum, representing metabolites, enzymes and proteins involved (**D-F**) Expression of dopamine markers in Aralar-KO striatum and limbic system. Representative Western blot of TH, DAT in striatum (**D**); and VMAT2, DARPP32

proteins in striatum (**E**) and limbic system (**F**) with their respective densitometric histograms. β-actin was used as charge control. Results are expressed as the mean ± s.e.m (n = 6 mice per group). Statistical analysis was performed by one-way ANOVA followed by Newman–Keuls test.* $p \leq 0.05$, ** $p \leq 0.01$, *** $p \leq 0.001$.

Figure 7- Mechanism for toxicity induced by the lack of Aralar in DAergic nigrostriatal nerve terminals. Lack of Aralar-MAS activity causes a decrease in mitochondrial NADH because both lack of redox transfer by the shuttle and limited pyruvate supply to mitochondria; and also decreased mitochondrial NAD(P)H content. Since glutathione system (and thioredoxin) for ROS detoxification is reduced by the mitochondrial NADPH pool; increased ROS is expected to happen in Aralar-deficient mitochondria. Mitochondrial ROS (O_2^- and H_2O_2) diffuse to the cytosol, provoking increased levels of cytosolic alpha-synuclein aggregates and synuclein-VMAT2 complexes in the presynaptic DA nerve terminals of Aralar-KO mice, with loss of VMAT2. Consequently, an increase in cytosolic DA produces an enhancement in DA autoxidation and in enzymatic oxidation via MAO activity (with higher DOPAC/DA ratio). Both pathways involve an overproduction of ROS, as reflected by increased GSSG, in Aralar-KO striatum. This further potentiates VMAT2 decline and possibly loss-of-function in the DA terminal with the subsequent mishandling of DA. AGC, aspartate-glutamate carrier; Asp, aspartate; AAT, aspartate aminotransferase; DA, dopamine; DOPAC, 3,4-dihydroxy-phenylacetic acid; G6P, glucose 6 phosphate; Glu, glutamate; Gluc, glucose; GA3P, glyceraldehyde 3-phosphate; GPx, glutathione peroxidase; GR, glutathione reductase; GSH, reduced glutathione ; GSSG, oxidized glutathione; α-KG; α-ketoglutarate; Lac, lactate; Mal, malate; MAO, monoamine oxidase; MDH, malate dehydrogenase; NNT, NADH-NADP-transhydrogenase; OAA,

oxalacetic acid; OGC, α-ketoglutarate-malate carrier; Pyr, pyruvate; VMAT2, vesicular monoamine transporter 2.

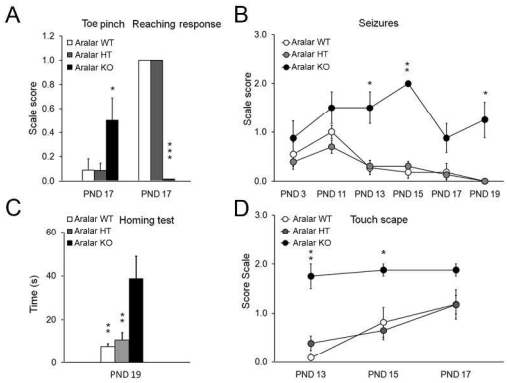

Llorente-Folch *et al*., Figure 1

199x279mm (300 x 300 DPI)

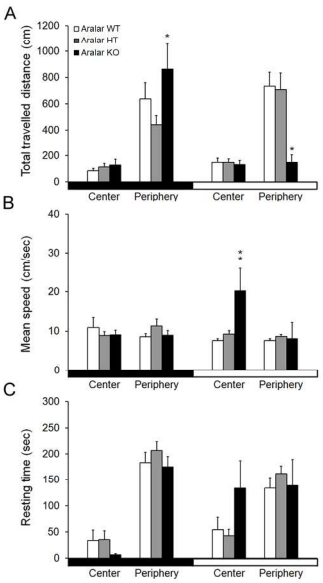

Llorente-Folch *et al.*, Figure 2

219x279mm (300 x 300 DPI)

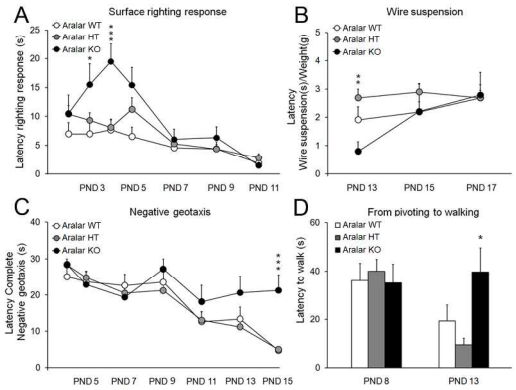

Llorente-Folch *et al.*, Figure 3

199x279mm (300 x 300 DPI)

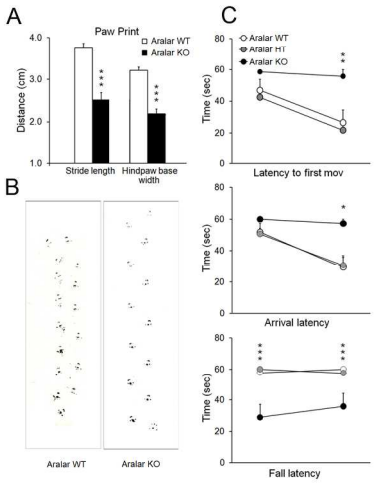

Llorente-Folch *et al.*, Figure 4

219x279mm (300 x 300 DPI)

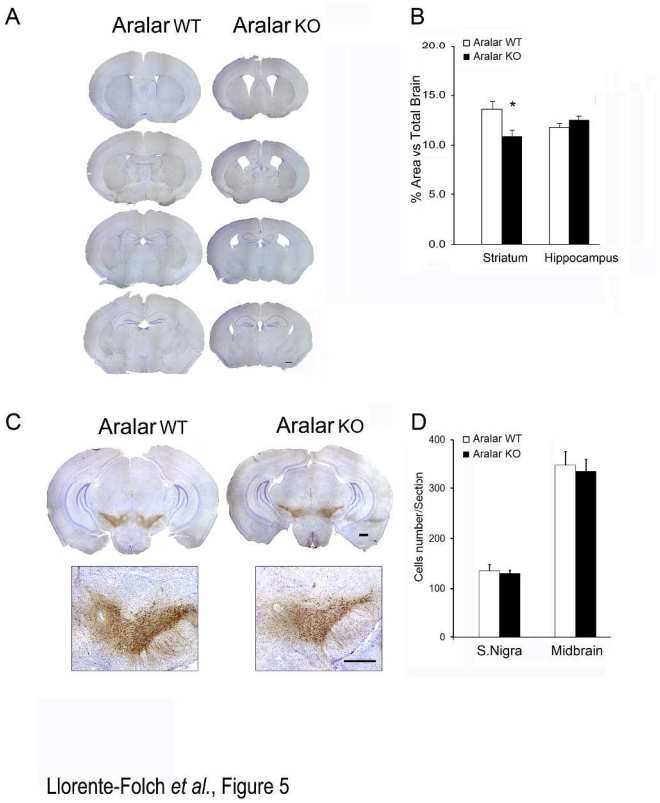

Llorente-Folch *et al.*, Figure 5

279x356mm (300 x 300 DPI)

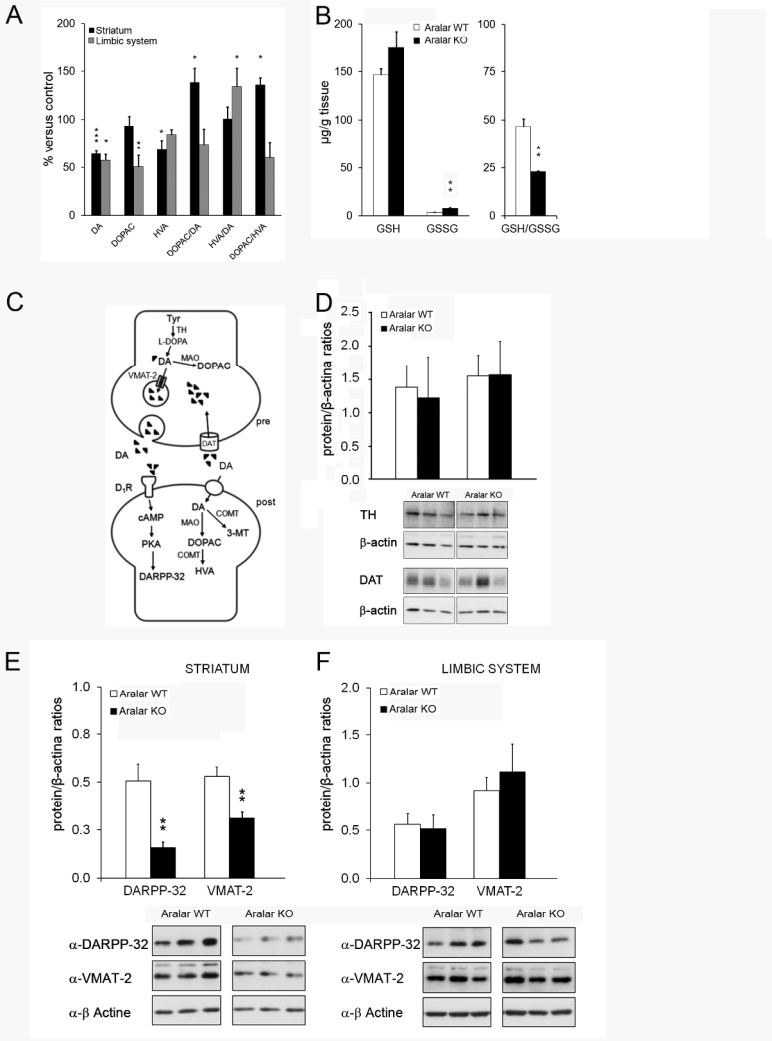

Llorente-Folch *et al.*, Figure 6

199x250mm (300 x 300 DPI)

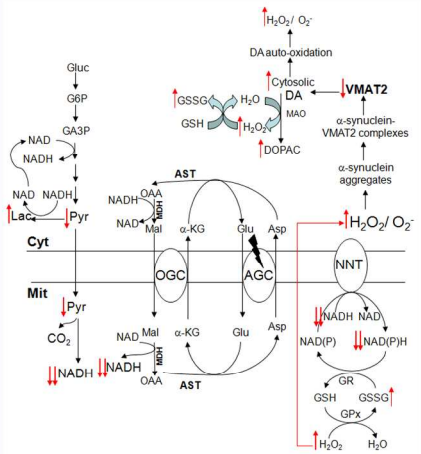

Llorente-Folch *et al*., Figure 7

199x250mm (300 x 300 DPI)

SUPPLEMENTARY INFORMATION

"AGC1-malate aspartate shuttle activity is critical for dopamine handling in the nigrostriatal pathway"

Irene Llorente-Folch[1], Ignasi Sahún[2], Laura Contreras[1], María José Casarejos[3], Josep María Grau[4], Takeyori Saheki[5], María Angeles Mena[3], Jorgina Satrústegui[1], Mara Dierssen[2], and Beatriz Pardo*[1]

MATERIALS AND METHODS

Animals

Male SVJ129 x C57BL6 mice carrying a deficiency for ARALAR expression (Aralar wild-type, WT; Aralar heterozygous, HT; and Aralar Knock-out, KO) were obtained from Lexicon Pharmaceuticals, Inc. (The Woodlands, TX, USA) (1). The mice were housed in a humidity- and temperature-controlled room on a 12-h light/dark cycle, receiving water and food *ad libitum*. Genotype was determined by PCR using genomic DNA obtained from tail or embryonic tissue samples (Nucleospin tissue kit, Macherey-Nagel) as described previously (Jalil *et al*., 2005). All the experimental protocols used in this study were approved by the local Ethics Committees at the Center of Molecular Biology "Severo Ochoa", Autónoma University (UAM), Madrid, and at the Center for Genomic Regulation, Barcelona.

General procedure for postnatal observations.

All the pregnant females were allowed to deliver spontaneously. Each pup was checked for gross abnormalities and the day after delivery was designated as PND1 of

age for neonates (estimation error on time of birth ± 8h). The pups were individually marked with ink and were nursed by their natural dams until weaning. During the testing protocol whole litters were separated from the dam less that 10 min and maintained in a warm environment. Males and females were pooled to perform the neurodevelopmental screening. All the measures were performed between 5:00 a.m and 8:00 a.m. All experiments procedures were approved by the Animal Care Committee of the Centre for Genomic Regulation. For the developmental screening 42 animals, males and females, were employed from five different litters.

Assessment of body growth

The pups were weighted daily from PND1 to PND5 and then every two days. The length of the body from the tip of the nose to the base of the tail and the length of the tail were recorded after determining the weight of the animals.

Developmental landmarks

The unit of analysis was the day of attainment of the criterion for each landmark. A brief description of each measure was as follows: 1) Pinna detachment: Pups were inspected for the complete separation of the pinna from the cranium from PND3. 2) Incisor eruption: Beginning on PND7, pups were inspected for the emergence of both lower and upper incisor from the gingiva. 3) Eye opening: Beginning on PND11, pups were inspected for the complete opening of both eyelids. 4) Permeation of ear conduct: Pups were inspected for opening of the auditory conduct.

Neurobehavioral development

Reflex and Sensory Function

Visual Placing: After the opening of the eyes, the pup was suspended by the tail and lowered towards the tip of a pencil without the vibrissae touching it, on PND17. The response was considered to be positive when the paws were extended to touch it.

Blast response: Exaggerated jumping or running behaviour in response to a gentle puff of air, on PND11.

Tactile Orientation: The test assessed the head turning (orienting) response triggered by the application to one side of the perioral area a cotton Q-tip, beginning on PND11.

Vibrissae Orientation: The pups were suspended by the tail and lowered towards the tip of a cotton Q-tip. At contact of the cotton with the vibrissae, the pup raised its head and performed a placing response, beginning on PND8.

Preyer reflex/Startle response: The response of the pups to a moderate sound burst consisting of a moderately brink flick of the pinna or startle response was recorded, beginning on PND11.

Toe Pinch: The test assessed the presence or absence of withdrawal answer against a mild painful stimulus, exerting pressure in a hind paw with the fingers, on PND17.

Reaching Response: The animal is held by the tail above a flat surface and it is noted if the forepaws are stretched out to make contact with the surface, on PND17.

Touch escape: Response of the animal to a finger stroke from above was recorded and scored, beginning on PND13, as follow: 0= no response, 1= moderate (rapid response to light stroke); and 2= vigorous (escape response to approach).

Convulsions: Spontaneous convulsions were recorded and scored as: 0= no convulsion, 1= moderate convulsion, 2= strong convulsion, in a longitudinal evaluation from PND3 onwards.

Neonatal Reflex and Acquisition

Root: After bilateral stimulation of the body, the pup was crawled forwards, pushing the head in a rooting fashion. We analyse the extinction of this archaic reflex from PND4 to PND8.

Crossed Extensor: When pinched, the stimulated limb flexed while the opposite limb extended. We analyse the extinction of this archaic reflex, from the very beginning to onwards.

Forepaw/Hindpaw Grasping: It was considered positive when the pup flexed the paw to grasp an object that was gently stroking it. The day of appearance of the reflex was recorded, starting on PND2.

Forpaw/Hindpaw Placing: When the dorsum of the paw or foot contact with the edge of an object, the hand or foot lifted and was placed on the object. It was recorded from PND4 to PND15.

Neuromotor Development

Surface righting response: The pup was placed on its back and the latency to turn over to rest in the prone position with all four feet on the floor was recorded (cut-off time 30 sec) starting the performance on PND4 until PND11.

Negative geotaxis test: The pups were placed head downward on a 45º incline and the latency to turn 180º was recorded, with a maximum latency of 30 sec, beginning on PND4 to PND15.

Wire suspension: The animals were forced to grasp a 3 mm-tick wire and hang from it on their forepaws. The ability of the animals to grasp the wire was scored and the time they held on the wire (maximum 30 sec) was registered. It was performed in PND13, 15 and 17 and latency to fall was correlated with the weight of the animal.

Walking/Pivoting: The latency for a mouse to lift up on all four paws and walk a distance exceeding its body length was measured on a flat surface covered with a paper, on PND8 and PND13.

Pivoting locomotion: The total number of degrees turned by the pup during a 60 sec period was recorded. The test was performed on a flat surface covered with a paper on which lines had been drawn to delineate four 90º quadrants. The number of degrees was scored only in completed 90º segments.

Homing Test

On PND19 individual pups were transferred to a cage containing new sawdust with a bite portion of sawdust of the home litter "goal arena". The pups were located at the opposite side of the goal arena, near to the wall. The time taken to reach the home litter sawdust was recorded (cut-off time 60 sec).

Paw Print test

To examine the step patterns of the hind limbs during forward locomotion, mice were required to traverse a straight, narrow tunnel. The experiments to evaluate the walking pattern of the mice were adapted from previous work by Martínez de Lagrán *et al.* (2004) and performed on PND18. The hind paws of the pups were coated with blue nontoxic waterproof ink. Animals were then placed at one end of a long narrow tunnel (10 X 10 x 30 cm), and in the opposite end there were placed part of their nest. They spontaneously enter and partially or totally traverse the tunnel. A clean sheet of white paper was placed on the floor of the tunnel to record the paw prints. The pattern of three consecutive steps (the first four steps were excluded from the analysis) was analysed and the following parameters assessed, averaged over consecutive steps:

(1) stride length, the averaged distance between each stride; (2) hindpaw base width, measured as the average distance between left and right hind footprint overlap. These values were determined by measuring the perpendicular distance of a given step to a line connecting its opposite preceding and proceeding.

Beam balance test

On PND19 individual pups were located in a trip of 40 X 2 cm elevated 25 cm from the surface. They began the task in the middle of the wooden trip and they should travel to reach the end of the trip with a cut-off time of 60 sec. Latency to the first movement, arrival latency and latency to fall were recorded. There was a first training session where the animals performed the task and learned about the mechanism. Mice were guided along the trip holding them by the tail to avoid any fall if they were not able to do it themselves. In a period of an hour the test was repeated, in this case without any help and counting the times.

Open field test

The open field was a white melamine box (70 × 70 × 50 cm high) divided into 25 equal squares and under high intensity light levels (high-lightening, 500 Lux) or in darkness (low-lightening, with weak red light). Mice tend to avoid brightly illuminated, novel, open spaces, so the open field environment acts as an anxiogenic stimulus and allows for measurement of anxiety-induced locomotor activity and exploratory behaviours. Thus, two zones, centre (1764 cm^2) and periphery (3136 cm^2) were delineated, being the centre more anxiogenic. At the beginning of the test session, mice at PND15-16 were left in the periphery of the apparatus and during 5 min we measured and analysed the latency to cross from the periphery to the centre, total

distance travelled, average speed and time spent in several sectors of the field (i.e. the border areas versus the open, central area). Observation was made in an actimeter (Panlab, Barcelona) by computerized analysis of movements.

Measurements of glutathione in brain regions

Total glutathione (Gsx) levels were measured by the method of Tietze (1969). A sample (40 μl) of the sonicated brain region supernatant in 0.4 N PCA was neutralized with four volumes of phosphate buffer (0.2 M NaH_2PO_4, 0.2 M Na_2HPO_4, 0.5 M EDTA, and pH 7.5). Fifty microlitres of this preparation were mixed with DTNB (0.6 mM), NADPH (0.2 mM) and glutathione reductase (1 unit) and the reaction was monitored in a P96 automatic microtiter reader at 412 nm for 6 min. Oxidized glutathione (GSSG) was measured as described by Griffith (1980). After the neutralization with the phosphate buffer, the sample remaining was mixed with 2-vinylpyridine (1.2 μl) at RT for 1 h and the reaction was carried out as described earlier. Reduced glutathione (GSH) was obtained by substracting GSSG levels from Gsx levels.

Histological and immunohistochemical studies in brain.

Animals were anesthetized by chloral hydrate (0.5 mg/g body weight; Sigma-Aldrich) and transcardially perfused with saline buffer (0.9% NaCl in phosphate buffer) and then with 4% formaldehyde in phosphate buffer (formalin fixative). Brains were carefully removed and postfixed overnight in formalin (4 ºC) and transferred into sucrose (30% in phosphate buffer). Later, they were embedded in OCT compound (Tissue-Tek ®, Sakura Finetek Europe B. V., Zoeterwoude, NL), frozen on dry ice and cut into 12 series of 30 microns coronal sections with a cryotome (free floating

sections). Sections were kept in cryoprotectant medium (25 % glycerol, 25 % ethylene glycol in 50 mM phosphate buffer) and stored at -20 ºC until processing.

For immunohistochemistry, sections were abundantly washed (1X PBS) and treated with $NaBH_4$ (1 mg/ml in PBS pH 8.0) to quench endogenous autofluorescence. Endogenous peroxidase was quenched in 3% H_2O_2 in 10% methanol in PBS for 20min, free-floating sections were blocked for 1h in PBS containing 10% normal horse serum, 0.25% Triton X-100 and incubated O/N at 4°C with antibodies against Tyrosine Hydroxilase (TH) (1:5000, polyclonal antibody, Millipore). Afterwards, sections were rinsed three times in PBS containing 0.25% Triton X-100 and then incubated for 2h with the secondary biotinylated antibody (goat-anti-rabbit, Vector, 1:150), followed by a 1h reaction with avidin-biotin peroxidase complexes (regular ABC kit Vectastain, Vector). After a profused wash with PBS containing 0.25% Triton X-100, sections were then developed using 0.05% 3,3-diaminobenzidine (Sigma) as a chromogen in the presence of 0.03% H_2O_2 in PBS and 8% NiCl for 2-10min. Sections were mounted onto poly-Lysine-coated slides, dehydrated, and coverslipped with DPX.

Cresyl Violet Immunostaining.

Cresyl Violet is a stain used for highlighting acidic components of tissue, called Nissl bodies in the neuronal cell; this is useful for determining structure in the cell. Sections (30 µm thick) were mounted on poly-Lysine covered slides and air dried at RT for several days. The staining procedure consists on sequentially dipping the slides in different solutions starting with absolute chloroform used as an organic lipid solvent for 30 min and continuing with 25% ethanol for 2min. Then, sections were submerged in stain (0.25% cresyl violet in 25% ethanol) for 5 min and subsequently in a series of

decreasing alcohol baths, 50% ethanol (30 sec) and 70% ethanol (5 min), dehydrating the samples. After 1 min in differentiation solution (70% ethanol, 10 drops of acetic acid), slides were soaked in 95% ethanol and finally in absolute ethanol for 1 min. Immunostaining was finished with 100% Xilene for 2 min and coverslipped with DPX mounting media letting them dry overnight.

Histomorphological studies of muscle

Muscle samples were frozen in cooled isopentane (liquid N_2) immediately after their obtaining. They were stored at -80ºC until sectioning in cryostat at -30ºC at 8-10 microns. The following histochemical reactions were performed: Hematoxilyn and eosin, (H&E), modified Gomori's trichrome for frozen tissue (TCR), non-specific esterase (NEE), Oil-red O, (ORO), NADH- tetrazolium reductase (NADH-TR), and ATP-ase at pH 9.4. The whole protocol for each reaction was that used in routine analysis of human muscle pathology and can be obtained elsewhere (Dubowitz and Sewry , 2007). Muscle biopsies were processed by an expert and blinded muscle pathologist (JMG).

Statistical analysis

For behavioral and motor tests, variance homogeneity and normality of data were tested by means of Levene and Shapiro–Wilk tests, respectively. Simple comparisons between genotypes mice were performed using the two-tailed unpaired Student´s t test with Whitney's correction to account for the different variances in the populations being studied. If the data did not meet specifications required for parametric analysis, non-parametric analysis of variance was used (Kruskal-Wallis) followed by comparisons between groups (Mann-Whitney U). Data were expressed as mean F SEM. In all tests,

a difference was considered to be significant if the obtained probability value was $P < 0.05$. These statistical analyses were performed with a commercial software package (Statistica 7.0).

Sample labeling and microarray hybridization

RNA purification

Mice (PND15) were sacrificed by cervical dislocation and brains were quickly extracted and frozen in liquid nitrogen. Total RNA was extracted using the RNeasy Tissue Kit (Quiagen), according to the manufacturer's instructions. RNA quantity was assessed using the NanoDrop-1000 (NanoDrop Technologies, Wilmington, DE), and RNA integrity was assessed by formaldehyde agarose gel electrophoresis. Samples with a discrete ribosomal 28S and 18S RNA bands and a 28S/18S intensity ratio of >2, and with a A260/A280 between 1.8-2.1 were used for amplification and labeling for microarray chip hybridization. Three independent RNA samples for each genotype were prepared and littermate pairs of Aralar-WT and Aralar-KO brains were processed and analyzed in parallel.

RNA amplification and labelling

One-Colour Microarray-Based Gene Expression Analysis Protocol (Agilent Technologies, Palo Alto, CA, USA) was used to amplify and label RNA. Briefly, 800 ng of total RNA was reverse transcribed using T7 promoter Primer and MMLV-RT. Then cDNA was converted to aRNA using T7 RNA polymerase, which simultaneously amplifies target material and incorporates cyanine 3-labeled CTP.

Hybridization protocol

Samples were hybridized to Whole Mouse Genome Microarray 4 x 44K (G4122F, Agilent Technologies). 1.65 μg of Cy3 labelled aRNA were hybridized for 17 hours at 65ºC in a hybridization oven (G2545A, Agilent) set to 10 rpm in a final concentration of 1X GEx Hybridization Buffer HI-RPM, according to manufacturer's instructions (One-Color Microarray-Based Gene Expression Analysis, Agilent Technologies).

Washing protocol

Arrays were washed according to manufacturer's instructions (One-Color Microarray-Based Gene Expression Analysis, Agilent Technologies). Arrays were dried out using a centrifuge.

Scan protocol

Arrays were scanned at 5μm resolution on an Agilent DNA Microarray Scanner (G2565BA, Agilent Technologies) using the default settings for 4x44k format one-colour arrays.

Image analysis

Images provided by the scanner were analyzed using Feature Extraction software (Agilent Technologies).

Data Analysis

Data files from Feature Extraction were imported into GeneSpring® GX software version 9.0. (Agilent Technologies). Quantile normalization was performed and expression values (log2 transformed) were obtained for each probe. Probes were also flagged (*Present*, *Marginal*, *Absent*) using GeneSpring® default settings. Probes with

signal values above the lower percentile (20th) and flagged as *Present* or *Marginal* in 100% of replicates in at least one out of the two conditions under study, were selected for further analysis (25517 probes).

In the next step, significance analysis of microarrays (SAM) (1) was used to identify differences in gene expression. Significance analysis of microarrays defines significance with the q value, an adjusted probability value for multiple comparisons. Statistical analysis of differential gene expression between KO and Wt (Control) was assessed using two-class paired SAM.

Ingenuity Pathway Analysis

Network, functional and pathway analyses of specific gene datasets were generated through the use of Ingenuity Pathway Analysis (Ingenuity Systems®, www.ingenuity.com).

The Functional analysis identified the functions and/or diseases that were most significant to the dataset. Genes from the dataset that were associated with biological functions and/or diseases in the Ingenuity knowledge base were considered for the analysis. Fischer's exact test was used to calculate a p-value determining the probability that each biological function and/or disease assigned to the data set is due to chance alone.

Canonical Pathway analysis identified the pathways from the Ingenuity Pathway Analysis library of canonical pathways that were more significant to the dataset. Genes associated with a canonical pathway in the Ingenuity knowledge base were considered for the analysis. The significance of the association between the dataset and the canonical pathway was measured in two ways: 1) A ratio of the number of genes from the dataset that map to the pathway divided by the total number of

molecules that exist in the canonical pathway is displayed. 2) Fisher's exact test was used to calculate a p-value determining the probability that the association between the genes in the dataset and the canonical pathway is explained by chance alone.

RESULTS

General development, neurodevelopment and psychomotor state is altered in Aralar-KO mice

Previously, we reported a significant growth retardation with premature death around PND21 Aralar-KO mice (1). Herein, a battery of neurodevelopmental, behavioral and motor tests were carried out to elucidate the specific problems related to AGC1-MAS deficiency, with special attention to motor deficits since an abnormal gait pattern was observed in Aralar-KO mice.

Aralar-KO mice have a reduced body and tail length from PND3, and a marked lower weight from PND5, never reaching normal growth compared to wild-type (WT) littermates **(data not shown).** In addition to their reduced size, Aralar-deficient mice suffer a delayed in the appearance of some developmental landmarks, incisor eruption, eyelid opening, permeation of the auditory conduct, and the functional measure associated with ear opening, the Preyer´s reflex (**not shown**). Acquisition of specific reflexes, such as hindpaw grasping and forepaw placing reflexes and extinction of archaic reflexes (rooting response and crossing extensor reflex) were also significantly delayed (**not shown**). Thus, although some phenotypic characteristics like pinna detachment and coat appearance occurred at the same time

than in WT mice, a general developmental delay was clearly present in Aralar-KO mice.

When performing the toe pinch test, Aralar-KO mice presented hyper-reactivity as compared to WT mice **(Fig. 1A**), but no alteration in the sensory tests was observed. The lack of Aralar caused a strong impairment in the reaching response capacity (**Fig. 1A)** in no case the forepaws were stretched out to make contact with the surface staying all the time in curling position. Aralar-KO animals showed a limb clasping phenotype, instead of showing a normal escape posture. This phenotype along with ataxia indicates severe alterations in the neurodevelopment possibly compromising cerebello-cortico-reticular and/or cortico-striato-pallido-reticular pathways (Takahaski *et al*., 2010; Lalonde and Straziele, 2011).

Spontaneous convulsions were observed in both WT and Aralar-KO mice at very early stages of development (from PND3; **Fig. 1B**), which gradually disappeared until complete extinction at PND15 in WT. However, in Aralar-KO mice, these convulsions neither disappeared nor decreased in intensity or frequency during development. Hyper-reactivity could also explain the results obtained in the touch escape test **(Fig. 1C**), where KO mice showed an exacerbated response to a finger stroke from above with no aversive effect in Aralar-WT or Aralar heterozygous (HT) mice.

No muscle affectation in Aralar-KO mice

Aralar is highly expressed in skeletal muscle (Jalil *et al.*, 2005) and its lack provokes motor disabilities in mice; thus, we have also studied the consequences of Aralar deficiency in skeletal muscle (**Fig. S1A, S1B**) No differences in fibre size were observed (H&E, **data not shown**) and TCR staining did not reveal myocytolysis, vacuolation or the presence of macrophages (**Fig. S1A**). In addition type I (oxidative)

and type II (glycolytic) muscle fibres, detected by NADH-TR method, were present in similar proportions in both groups of animals **(Fig. S1B)**. ATPase activity (by histochemistry) was also detected in both genotypes, although with less intensity for Aralar-KO (**not shown**). In conclusion, no histomorphological abnormalities or signs of pathology were detected in the gastronemius muscle of Aralar-KO mice at PND20.

REFERENCES

Dubowitz V, Sewry C (2007): Muscle biopsy. A practical Approach, 3rd edn. W.B. Saunders/Elsevier, London, Philadelphia, pp. 21-39.

Griffith, O.W., 1980. Determination of glutathione and glutathione disulfide using glutathione reductase and 2-vinylpyridine. Anal. Biochem. 106, 207-212.

Jalil MA, Begum L, Contreras L, Pardo B, Iijima M, Li MX *et al*. (2005): Reduced *N*-acetylaspartate levels in mice lacking Aralar, a brain- and muscle-type mitochondrial aspartate-glutamate carrier" *J. Biol. Chem.* **280**: 31333-31339.

Lalonde R, Straziele C (2011): Brain regions and genes affecting limb-clasping responses. *Brain Res. Rev*. **67**: 252-259.

Martínez de Lagrán M, Altafaj X, Gallego X, Martí E, Estivill X, Sahún I, Fillat C, Dierssen M (2004): Motor phenotypic alterations in TgDyrK1a transgenic mice implicate DYRK1A in Down syndrome motor dysfunction. *Neurobiol Disease* **15**: 132-142.

Takahaski E, Niimi K, Itakura C (2010): Neonatal motor functions in Cacna1α mutant rolling Nagoya mice. *Behav. Brain Res*. 207: 273-279.

Tietze, F., 1969. Enzymatic method for quantitative determination of nanogram amounts of total and oxidized glutathione: application to mammalian blood and other tissues. Anal. Biochem. 27, 502-522.

Legend to Figure:

Figure S1- (**A-B**) Representative images of muscle sections obtained from gastronemius of Aralar-KO and WT mice at 20 PND stained with TCR (**A**) and NADH-TR (**B**). Histomorphology revealed by these techniques show no remarkable differences between genotypes. (n=4). Scale bar, 40 μm.

Figure S2- The content of GSH and GSSG was not significantly different in limbic sytem (**A**) and brainstem (**B**) of Aralar KO mice as compared to Aralar WT. GSH/GSSG ratios were unchanged between genotypes in both regions (A and B). Results are expressed as the mean ± s.e.m (n = 6 mice per group).

Table S1-Enzymes with a significant 2-fold increase or reeduction in the Aralar-KO mouse

Name	Ratio (KO/WT)	q-value	Description	Pathway	Disease
GAMT	0.49448546	0.01301	guanidinoacetate N-methyltransferase	Aminoacid metabolism: Arginine, proline, serine, glycine and threonine	
MAOB	0.51619927	0.01787	monoamine oxidase B	Catecholamine catabolism, aminoacid metabolism (Arg, Pro, Ser, gly, Thre, Trp, Tyr)	
PRODH	0.47565914	0.01787	proline dehydrogenase (oxidase) 1	Arg, Pro mtb.	hyperprolinemia and neurological disorder.
SDS	0.33868124	<0.005	serine dehydratase	Ser, gly, Thr, Trp mtb, Lys degradation	
CYP4F8	0.35527301	0.00659	cytochrome P450, family 4, subfamily F, polypeptide 8	Trp mtb, Arachidonic acid mtb.	
DCT	0.41151017	0.00659	dopachrome tautomerase (dopachrome delta-isomerase, tyrosine-related protein 2)	Tyr mtb	
AASS	0.39639207	<0.005	aminoadipate-semialdehyde synthase	Lys degradation	
ALOX5	0.48632747	0.00689	arachidonate 5-lipoxygenase	Arachidonic acid mtb	
PLA2G4A	0.46878555	0.01301	phospholipase A2, group IVA (cytosolic, calcium-dependent)	Arachidonic acid mtb	neurological disorder
PROCA1	2.24388696	0.01567	proline-rich cyclin A1-interacting protein	Arachidonic acid mtb	
ACSS2	0.65022007	0.0415	acyl-CoA synthetase short-chain family member 2	glutathione mtb	
GPX6	0.56840849	0.04059	glutathione peroxidase 6 (olfactory)	glutathione mtb	
GSTM1	1.98894034	0.04059	glutathione S-transferase, mu 1	glutathione mtb	
LNPEP	0.54676773	0.00659	leucyl/cystinyl aminopeptidase	glutathione mtb	
MGST1	1.90924203	0.02504	microsomal glutathione S-transferase 1	glutathione mtb	

Microarray comparison of wt and aralar KO was carried out as stated in the Material and method section. This table shows the relevant enzymes with a significant increase or decrease (Significance Analysis of Microarrays, q-value lower than 0.05, a 2-fold alteration in mRNA levels) in the glutathione and aminoacid metabolism, as obtained by ingenuity pathway analysis software.

Table S2- Demyelination-related genes

Name	Ratio (KO/WT)	q.value	Description	Pathway	Disease
ASPA	0.42103148	0.00659	aspartoacylase	Asp, ala mtb, Canavan's disease	
Mobp	0.26169276	0.00659331	myelin-associated oligodendrocytic basic protein [NM_008614]		
Mal	0.27181954	< 0,005	myelin and lymphocyte protein, T-cell differentiation protein (Mal), mRNA [NM_010762]		neurological disorder
Mag	0.3906884	< 0,005	myelin-associated glycoprotein (Mag), mRNA [NM_010758]		neurological disorder
Plp1	0.4099373	0.0130072	proteolipid protein (myelin) 1 (Plp1), mRNA [NM_011123]		neurological disorder
Mog	0.43395389	0.01712291	myelin oligodendrocyte glycoprotein (Mog), mRNA [NM_010814]		neurological disorder
Mbp	0.56516966	0.04149798	myelin basic protein (Mbp), transcript variant 7, mRNA [NM_010777]		
ccl3			(demyelination nervous tissue)		

Microarray comparison of wt and aralar KO was carried out as stated in the Material and method section. This table shows the relevant proteins with a significant increase or decrease (Significance Analysis of Microarrays; q-value lower than 0.05, a 1.8 fold alteration in mRNA levels) involved in the myelinization process, as obtained by ingenuity pathway analysis software.

Table S3-Aminoacid and metabolite transport

Name	Ratio (KO/WT)	q-value	Description	Pathway	
Slc6a4	5.55695907	0.02761398	Neurotransmitter transporter, serotonin		
Slc3a2	2.34417908	0.02761398	activators of dibasic and neutral amino acid transport	Transport of essential aminoacids	
Slc15a3	2.30898427	0.01576956	Slc15a3	Proton-dependent oligopeptide trasnporter	
Slc7a11	2.30802488	0.00516773	cationic amino acid transporter, y+ system; cysteine/glutamate transport	Production of glutathione	
Slc7a3	2.26990244	0.01576956	cationic amino acid transporter, y+ system	Incorporation of arginine, incorporation of basic aminoacid, transport of essential aminoacids	
Slc1a4	1.76166806	0.04058765	glutamate/neutral amino acid transporter	Transport of neutral aminoacids	
Slc44a1	0.55988432	0.01712291	solute carrier family 44, member 1	Choline trans membrane transporter activity	
Slc34a3	0.47545072	0.0250446	sodium phosphate		
Slc25a21	0.43614698	0.01712291	mitochondrial oxodicarboxylate carrier	Alpha-ketoglutarate transport	
Slc35b3	0.39878825	0.00659331	Mus musculus 16 days neonate thymus cDNA, RIKEN full-length enriched library, clone:A130081B15 product:unclassifiable, full insert sequence. [AK079504]	Adenosine 3'-phospho 5' phosphosulfate transporter 2	
Slc45a3	0.29398712	<0.005	solute carrier family 45, member 3		
Slc25a12	0.00768092	<0.005	Mus musculus solute carrier family 25 (mitochondrial carrier, Aralar), member 12 (Slc25a12), mRNA [NM_172436]	Production of aspartate, malate aspartate shuttle, mylein production	
SLC25A13	4.14979757		solute carrier family 25, member 13 (citrin)	Malate aspartate shuttle, urea cycle	Type II citrulinemia

Microarray comparison of wt and aralar KO was carried out as stated in the Material and method section. This table shows the relevant carriers with a significant increase or decrease (Significance Analysis of Microarrays , q-value lower than 0.05, a 2-fold alteration in mRNA levels involved in the aminoacid and metabolite transport, as obtained by ingenuity pathway analysis software

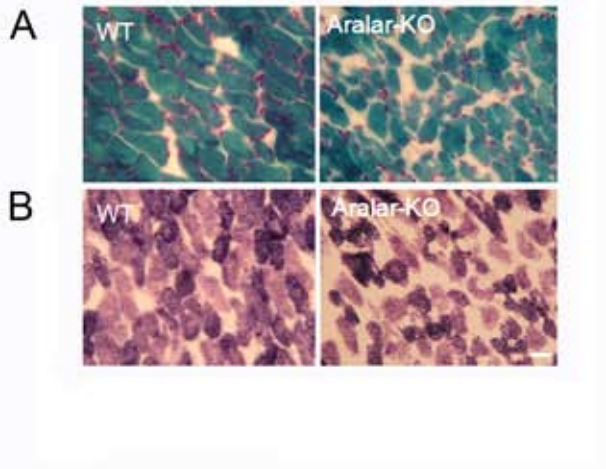

Llorente-Folch I *et al.*, Supplementary 1

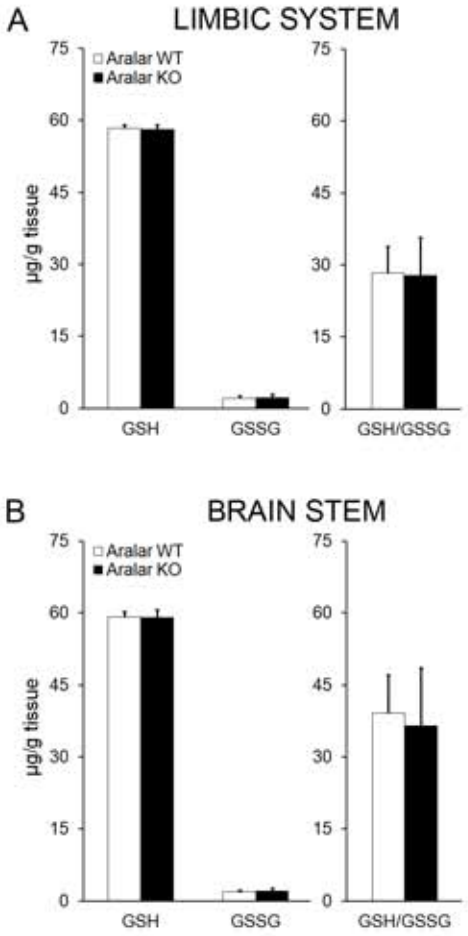

Llorente-Folch *et al.*, Supplementary 2